RESEARCH PAPER

Naringin directly activates inwardly rectifying potassium channels at an overlapping binding site to tertiapin-Q

Tin T Yow[1], Elena Pera[1], Nathan Absalom[1], Marika Heblinski[2], Graham AR Johnston[3], Jane R Hanrahan[1] and Mary Chebib[1]

[1]*Faculty of Pharmacy, The University of Sydney, Sydney, NSW, Australia,* [2]*Northern Clinical School, The University of Sydney, Sydney, NSW, Australia, and* [3]*Department of Pharmacology, The University of Sydney, Sydney, NSW, Australia*

BACKGROUND
G protein-coupled inwardly rectifying potassium ($K_{IR}3$) channels are important proteins that regulate numerous physiological processes including excitatory responses in the CNS and the control of heart rate. Flavonoids have been shown to have significant health benefits and are a diverse source of compounds for identifying agents with novel mechanisms of action.

EXPERIMENTAL APPROACH
The flavonoid glycoside, naringin, was evaluated on recombinant human $K_{IR}3.1$–3.4 and $K_{IR}3.1$–3.2 expressed in *Xenopus* oocytes using two-electrode voltage clamp methods. In addition, we evaluated the activity of naringin alone and in the presence of the $K_{IR}3$ channel blocker tertiapin-Q (0.5 nM, 1 nM and 3 nM) at recombinant $K_{IR}3.1$–3.4 channels. Site-directed mutagenesis was used to identify amino acids within the M1–M2 loop of the $K_{IR}3.1^{F137S}$ mutant channel important for naringin's activity.

KEY RESULTS
Naringin (100 µM) had minimal effect on uninjected oocytes but activated $K_{IR}3.1$–3.4 and $K_{IR}3.1$–3.2 channels. The activation by naringin of $K_{IR}3.1$–3.4 channels was inhibited by tertiapin-Q in a competitive manner. An alanine-scan performed on the $K_{IR}3.1^{F137S}$ mutant channel, replacing one by one aromatic amino acids within the M1–M2 loop, identified tyrosines 148 and 150 to be significantly contributing to the affinity of naringin as these mutations reduced the activity of naringin by 20- and 40-fold respectively.

CONCLUSIONS AND IMPLICATIONS
These results show that naringin is a direct activator of $K_{IR}3$ channels and that tertiapin-Q shares an overlapping binding site on the $K_{IR}3.1$–3.4. This is the first example of a ligand that activates $K_{IR}3$ channels by binding to the extracellular M1–M2 linker of the channel.

Abbreviations
CGP36742 or SGS742, 3-aminopropyl-*n*-butylphosphinic acid; GPCRs, G protein-coupled receptors; $K_{IR}3$, G protein-coupled inwardly rectifying potassium channels; LPA, lysophosphatidic acid; PIP_2, phosphatidylinositol 4,5-bisphosphate; r $K_{IR}1.1$, rat renal outer medullary potassium; TPN-Q, tertiapin-Q

Introduction

G protein-coupled inwardly rectifying potassium channels ($K_{IR}3$/GIRK) are members of a family of inwardly rectifying potassium channels. These channels are activated by G protein-coupled receptors (GPCRs) such as opioid, adenosine, muscarinic, $GABA_B$ and dopamine receptors (Ikeda *et al.*, 1995; 1996; 1997; Luscher *et al.*, 1997). Four subunits have

been identified termed $K_{IR}3.1$–3.4 (Lesage *et al.*, 1994). In general, heterotetrameric channels are formed by $K_{IR}3.1$ coupling to either $K_{IR}3.2$ or $K_{IR}3.4$ subunits resulting in the formation of $K_{IR}3.1$–3.2 channels (present mainly in brain regions) (Kobayashi *et al.*, 1995; Lesage *et al.*, 1995) and $K_{IR}3.1$–3.4 channels (present mainly in the heart and endocrine regions) (Corey and Clapham, 1998; Gregerson *et al.*, 2001). Such channels play an important role in regulating neuronal excitability and heart rate (Signorini *et al.*, 1997; Wickman *et al.*, 1998).

The activation of $K_{IR}3$ channels involves many intrinsic factors including Mg^{2+} and Na^+, pH, phosphatidylinositol 4,5-bisphosphate (PIP_2) and intracellular proteins such as $G_{i/o}$ proteins (Nichols and Lopatin, 1997; Mark and Herlitze, 2000). Hormones, transmitters and peptides indirectly activate $K_{IR}3$ channels by preferentially stimulating *Pertussis* toxin-sensitive GPCRs (Sadja *et al.*, 2003) causing the $G\alpha$ subunit to replace its bound GDP with GTP. This causes the $G\beta\gamma$ subunit to dissociate from the $G\alpha$ subunit, which in turn directly binds and activates the GIRK channel at several intracellular sites on the N- and C-termini (Lesage *et al.*, 1994; Nishida and MacKinnon, 2002). The activation of $K_{IR}3$ channels by the $G\beta\gamma$ subunit in turn stabilizes PIP_2 interactions (Sui *et al.*, 1998; Logothetis and Zhang, 1999) and is accelerated by some members of the regulators of G protein signalling family of proteins (Dascal, 1997; Mark and Herlitze, 2000; Sadja *et al.*, 2003). Finally the activation signal is terminated when $G\alpha$-GTP is hydrolysed back to $G\alpha$-GDP, which enables the $G\beta\gamma$ subunit to associate and reform the $G_{i/o}$ trimer. Some members of the regulators of G protein signalling family of proteins also contribute to this process, paradoxically also accelerating the deactivation kinetics (Benians *et al.*, 2005).

A number of direct inhibitors of $K_{IR}3$ channels have been reported including some opioids (Ulens *et al.*, 1999), antipsychotics and antidepressants (Kobayashi *et al.*, 2000; 2003; 2004), and the bee toxin, tertiapin-Q (Jin *et al.*, 1999). In contrast, only ethanol (Kobayashi *et al.*, 1999; Lewohl *et al.*, 1999) and halothane (Weigl and Schreibmayer, 2001; Yamakura *et al.*, 2001) have been reported to directly activate the channels.

Flavonoids are natural polyphenolic agents found in all plants (Mattila *et al.*, 2000). They are secondary metabolites, which are consumed in significant amounts from beverages, fruits and vegetables. Flavonoids have been shown to have significant health benefits (Birt *et al.*, 2001) being involved in a variety of biological processes. They have been shown to reduce heart disease (Renaud and de Lorgeril, 1992), be protective against cancers (Kandaswami *et al.*, 1991; Hertog *et al.*, 1995) and neurodegenerative diseases such as Alzheimer's disease (Mandel and Youdim, 2004). Thus, flavonoids are a diverse source of compounds for identifying agents with novel mechanisms of action.

Naringin and its aglycosylated analogue ($\pm$)-naringenin are bioflavanoids found in grapefruit. Both agents have a chiral centre at the C2 position of the middle ring (Figure 1) resulting in two stereoisomers. Both enantiomers are found naturally in the fruit and contribute to the fruits' bitter flavour. In this study, we evaluated the effects of naringin (racaemic mixture) and ($\pm$)-naringenin on recombinant wild-type and mutant $K_{IR}3$ channels expressed in *Xenopus* oocytes.
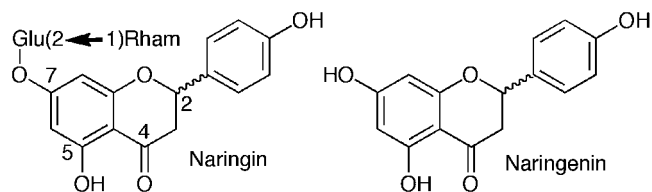

Figure 1

Structures of naringin and naringenin.

The data show that naringin but not ($\pm$)-naringenin activates $K_{IR}3$ channels. The activation is inhibited by low nanomolar concentrations of tertiapin-Q in a competitive manner indicating a common or overlapping binding site on the $K_{IR}3$ channel. Site-directed mutagenesis studies replacing aromatic amino acids [phenylalanine (Phe) and tyrosine (Tyr)] located on the extracellular linker that connects the intracellular transmembrane domains 1 and 2 (M1–M2 linker) of the homotetrameric $K_{IR}3.1^{F137S}$ mutant channel to alanine (Ala) identified Tyr148 and Tyr150 as important for naringin's affinity. This is the first report of a molecule that binds to the extracellular vestibule of the $K_{IR}3$ channel and triggers channel opening.

Methods

Materials

Naringin ($\pm$)-naringenin, barium chloride ($BaCl_2$), adenosine, theophylline and LPA were obtained from Sigma, Australia. Neohesperidose was obtained from ABCR GmbH& Co. KG, Karlsruhe, Germany. 3-Aminopropyl-*n*-butylphosphinic acid (CGP36742 or SGS742) was a gift from Dr Wolfgang Froestl (formerly Novartis, Switzerland).

Rat $K_{IR}3.4$, human $GABA_{B(1b)}$ and $GABA_{B2}$ subcloned in pcDNA3.1(–), and rat $K_{IR}3.1$ subcloned in pBluescript were gifts from Drs Fiona Marshall and Andrew Green (Glaxo Wellcome, UK). Human $K_{IR}3.1$ and $K_{IR}3.2$ subcloned into pCMV6-XL5 and pCMV6-XL4 were obtained from Origene Technologies, Inc., MD, USA.

Molecular biology

Human $GABA_{B(1b)}$ and $GABA_{B2}$ cDNAs were linearized using EcoRI. Human $K_{IR}3.1$, rat $K_{IR}3.1$ and $K_{IR}3.4$ cDNAs were linearized with XbaI. Human $K_{IR}3.2$ cDNA was linearized with SmaI and SacI and the DNA extracted *via* QIAquick gel extraction kit (QIAGEN Pty Ltd, Australia). mRNAs were transcribed *in vitro* using T7 mMessage mMachine transcription kit (Ambion Inc., Austin, TX, USA) for all linearized cDNAs.

For $K_{IR}3.1$–3.4 and $K_{IR}3.1$–3.2 channel expression, the mRNA ratio injected was 1:1 with a total RNA concentration of 100 and 80 ng per oocyte respectively. For $GABA_B$-$K_{IR}3$ receptor expression, the mRNA ratios used for $GABA_{B(1b)}$: $GABA_{B2}$: $K_{IR}3.1$: $K_{IR}3.4$ were 1:2:1:1 with a total RNA concentration of 80 ng per oocyte. For $GABA_B$-$K_{IR}3$ mutant expression, the mRNA ratio was 1:2:1 [$GABA_{B(1b)}$: $GABA_{B2}$: mutant] and the RNA concentration

ranged between 40 and 130 ng per oocyte. For expressing $K_{IR}3$ mutations alone, the final concentration used was 25 ng per oocyte.

Electrophysiological recording

Animal ethics approval was granted by The University of Sydney Animal Ethics Committee and followed the NH&MRC guidelines on the Australian code of practice for the care and use of animals for scientific research (L24/2–2006/3/4267). In brief, female *Xenopus laevis* were anaesthetized with tricaine (850 mg·500 mL^{-1}). Several ovarian lobes were surgically removed by a small incision on the abdomen of the *X. laevis*. The lobes were cut into small pieces and were rinsed thoroughly with oocyte releasing buffer 2 [OR2; 82.5 mM NaCl, 2 mM KCl, 1 mM MgCl$_2$, 5 mM HEPES (hemi-Na)]. The lobes were digested with collagenase A (2 mg·mL^{-1} in OR2; Boehringer Manheim, Germany) at room temperature. The oocytes were further washed with OR2 and stored in ND96 wash solution [96 mM NaCl, 2 mM KCl, 1 mM MgCl$_2$, 1.8 mM CaCl$_2$, 5 mM HEPES (hemi-Na)] supplemented with 2.5 mM sodium pyruvate and 0.5 mM theophylline until ready for injection. Stage V–VI oocytes were selected and microinjected with 50.6 nL of mRNA. After injection, the oocytes were maintained at 18°C in the presence of ND96 wash solution augmented with 2.5 mM sodium pyruvate, 0.5 mM theophylline and gentamicin at 50 µg·mL^{-1}.

Naringin was stored at 500 mM stock in DMSO and (±)-naringenin was stored as 100 mM in DMSO at –20°C. Prior to recording, the compounds were diluted with either: (i) 45 mM K$^+$ buffer: 45 mM NaCl, 45 mM KCl, 1 mM MgCl$_2$, 1.8 mM CaCl$_2$, 5 mM HEPES (hemi-Na salt); or (ii) 90 mM K$^+$ buffer: 90 mM KCl, 1 mM MgCl$_2$, 1.8 mM CaCl$_2$, 5 mM HEPES (hemi-Na salt) to the desired concentration with a final concentration of DMSO equal to 0.8%.

Whole-cell currents were measured using a two-electrode voltage clamp set-up composed of a Digidata 1200, Geneclamp 500B amplifier and pClamp 8 (Axon Instruments Inc., Foster City, CA, USA), together with a Powerlab/200 (AD Instruments, Sydney, Australia) and Chart version 5.5 program for PC. Voltage was maintained at –60 mV. For current–voltage analysis, the holding potential was –30 mV and currents were measured from –80 mV to 60 mV in 10 mV increments in response to 100 ms voltage steps. This measurement was performed after a 2 min perfusion of each of the following buffers: ND96, 45 mM K$^+$, 90 mM K$^+$, naringin (100 µM) in 45 and 90 mM K$^+$ buffers for GIRK1/4 and ND96, 45 mM K$^+$, naringin (100 µM) in 45 mM K$^+$ buffer for $K_{IR}3.1$–3.2 and mutant channels. Traces recorded in ND96 were subtracted offline from traces recorded under the various buffers in order to correct for leak and endogenous oocyte currents.

The recording microelectrodes were filled with 3 M KCl [or 3 M KCl and 11 mM ethylene glycol tetraacetic acid (EGTA)] and the resistance was between 0.2 and 1.0 mΩ. Two to five days post injection, oocytes were used for recording. Oocytes were initially superfused with ND96 until a stable base current was achieved at which point the buffer was switched to a high K$^+$ buffer (45 or 90 mM K$^+$). Compounds were only applied once a stable base current was reached. A 6 min wash period was applied between drug applications.

Evaluating the effect of naringin at intracellular sites of GIRK1/4 channels

Oocytes expressing $K_{IR}3.1$–3.4 and responding to extracellularly applied naringin (100 µM) or ethanol (100 mM) were further injected with 50.6 nL of water (control), ethanol (2 M) (positive control) or naringin (2 mM) (note: as the volume of a single oocyte is ~1 µL, the final intracellular concentration of ethanol and naringin were ~100 mM and ~100 µM respectively). The effects on the whole-cell currents were monitored for up to 40 min.

Binding studies

Naringin (10 µM) was tested on a series of primary binding assays performed by the National Institute of Mental Health's Psychoactive Drug Screening Program, Contract # NO1MH32004 (NIMH PDSP) directed by Bryan L. Roth MD, PhD at the University of North Carolina at Chapel Hill and Project Officer Jamie Driscol at NIMH, Bethesda MD, USA. For experimental details please refer to the PDSP web site http://pdsp.med.unc.edu/.

Site-directed mutagenesis studies

Sense and antisense oligonucleotide primers (Table S1) were designed to introduce the point mutations within the $K_{IR}3.1$ and $K_{IR}3.4$ subunits. Phenylalanine (Phe; F) 137 of the $K_{IR}3.1$ subunit was mutated to serine (Ser; S) while Ser143 of the $K_{IR}3.4$ subunit was mutated to threonine (Thr; T) in order to form the homotetrameric channels $K_{IR}3.1^{F137S}$ and $K_{IR}3.4^{S143T}$ (Chan *et al.*, 1996). Using the $K_{IR}3.1^{F137S}$ subunit, a series of secondary mutations were performed replacing either tyrosine (Tyr; Y) or Phe in the M1–M2 linker to alanine (Ala; A) using the QuikChange Site-Directed Mutagenesis Kit (Stratagene, La Jolla, CA, USA). DNA plasmids containing the singly or doubly mutated $K_{IR}3.1^{F137S}$ subunit were transformed into XL1-Blue supercompetent cells (Stratagene, CA, USA) and cultured in LB broth with ampicillin (5 µg·mL^{-1}). Successful mutants were identified by restriction enzyme analysis and verified by DNA sequencing. The mRNA of the single and double mutations were expressed in oocytes alone or in the presence of the GABA$_{B(1b,2)}$ receptor before evaluating with naringin, adenosine or GABA.

Statistical analysis

Data are represented as the mean (±SEM) from a specified number of independent experiments or as mean (95% CI). For the concentration–response curves, data points were fitted using GraphPad Prism 5. The current was normalized to the maximum concentration of agonist in the following ratio (I/I_{max}) unless otherwise stated. The concentration–response curves were plotted using current ratios (*Y*-axis) and plotted against log of the concentration (*X*-axis) and fitted to the following formula:

$$I = I_{max}[A]^{n_H}/(EC_{50}{}^{n_H} + [A]^{n_H}) \text{ (Miller, 2003)}$$

Where, I = current response, I_{max} = maximum current, n_H = Hill slope and [A] = agonist concentration.

The binding constant for antagonist (K_b) was estimated using the Schild equation $K_b = (\{A\}/\{A*\}-1) - [Ant]$, where $\{A\}$

is the EC_{50} of agonist in the presence of antagonist, {A*} is the EC_{50} of agonist in the absence of antagonist, [Ant] is the concentration of antagonist, and simple competitive antagonism (m = 1) is shown by plotting the log (dose ratio − 1) versus −log [Ant].

Statistical analyses were performed using a one-way ANOVA followed by Tukey's multiple comparison *post hoc* test when comparing multiple groups (unless otherwise stated) or with a paired Student's *t*-test when comparing two groups. Statistical probability (*P*) are expressed as *P < 0.05, **P < 0.01 and ***P < 0.001.

Nomenclature

The nomenclature of all molecular targets (receptors, ion channels, enzymes, etc.) cited in this work conforms to the British Journal of Pharmacology's Guide to Receptors and Channels (Alexander *et al.*, 2009).

Results

High concentrations of naringin activate endogenous K^+ channels and calcium-activated chloride channels in Xenopus *oocytes*

In the presence of high K^+ buffers (45 or 90 mM K^+ buffers) to increase the K^+ driving force at the holding potential (−30 mV), small basal currents were observed in uninjected oocytes (10–30 nA), indicating the presence of endogenous potassium channels. When naringin ($\geq$100 μM) was added to uninjected cells, a small response ($\leq$10–20 nA) was detected in the presence of 45 mM K^+ buffer. As naringin is reported to weakly activate Ca^{2+}-activated K^+ channels (BK_{Ca}) (Saponara *et al.*, 2006) and *Xenopus* oocytes are known to express an endogenous homologue of these channels, it was thought that naringin may be activating these channels (Kanjhan *et al.*, 2005). In addition, naringin ($\geq$100 μM) elicited a sharp current indicative of activating the endogenous Ca^{2+}-activated Cl^- channel in both ND96 and 45 mM K^+ buffer (Figure S1) and the levels of each varied with individual cells. Therefore for subsequent experiments, intracellular Ca^{2+} was buffered with 11 mM EGTA in the recording microelectrode and was allowed to equilibrate in the oocyte for 15 min prior to recording. In addition, oocytes injected with $K_{IR}3$ channels were stored at 4°C for 24–48 h prior to use as this treatment helped reduce the expression of the unwanted Ca^{2+}-activated Cl^- channels [modified from (Varecka and Peterajova, 1990)]. Any oocytes that responded with a sharp inward current typical of Ca^{2+}-activated Cl^- channel activity were discarded.

Naringin but not (±)-naringenin activates $K_{IR}3$ channels

In oocytes expressing $GABA_B$ receptors and $K_{IR}3.1$–3.4 channels, both GABA (100 μM and 3 μM) and naringin (100 μM) activated the channel (Figure S2A). The effect of GABA (3 μM) but not naringin (100 μM) was blocked by the competitive $GABA_{B/C}$ receptor antagonist, CGP36742 100 μM (Figure S2B),

indicating the activation of the $K_{IR}3$ channel by naringin is not via the $GABA_B$ receptor. Furthermore, naringin (100 μM) but not (±)-naringenin (100 μM) or the C7 sugar moiety of naringin, neohesperidose (100 μM) activated oocytes expressing $K_{IR}3.1$–3.4 and $K_{IR}3.1$–3.2 channels (Figure S2B & S2C).

Naringin activates $K_{IR}3$ channels independently of the extracellular K^+ concentration

In oocytes expressing only $K_{IR}3.1$–3.4 channels, upon switching buffer solutions from ND96 to 45 mM K^+, basal currents of the order 313 ± 37 nA (*n* = 71) were generated. Naringin (100 μM) further activated the channel by 240 ± 22 nA (*n* = 71). In the presence of 90 mM K^+ buffer, basal currents increased compared with 45 mM K^+ buffer and were of the order 1406 ± 340 nA (*n* = 17). Naringin (100 μM) further increased the current by 949 ± 120 nA (*n* = 17). An example of the current produced by naringin (100 μM) in the presence of 45 and 90 mM K^+ buffers at $K_{IR}3.1$–3.4 is shown in Figure 2. The current–voltage relationship in the presence and absence of naringin (100 μM) using 45 and 90 mM K^+ buffers at $K_{IR}3.1$–3.4 is also shown in Figure 2B. Under these conditions, the response of $K_{IR}3.1$–3.4 to 45 and 90 mM K^+ is strongly rectified. Naringin (100 μM) further activates the channel and this effect is voltage-independent.

In oocytes expressing only $K_{IR}3.1$–3.2, the basal currents produced in the presence of 45 and 90 mM K^+ buffers were 583 ± 71 nA (*n* = 50) and 823 ± 127 nA (*n* = 23) respectively. Naringin (100 μM) further increased the currents by 207 ± 25 nA (*n* = 38) and 505 ± 194 nA (*n* = 23) respectively.

Table 1 summarizes the activity of naringin at $K_{IR}3.1$–3.4 and $K_{IR}3.1$–3.2 under various conditions. Figure 2C and D shows an example of the responses in an oocyte expressing $K_{IR}3.1$–3.4 and $K_{IR}3.1$–3.2 respectively. Naringin dose-dependently activated these channels. The EC_{50} for naringin at $K_{IR}3.1$–3.4 and $K_{IR}3.1$–3.2 channels in the presence of 45 mM K^+ were not significantly different (*P* > 0.05; one way ANOVA, followed by Tukey's multiple comparison test; Table 1). The EC_{50} values for naringin at $K_{IR}3.1$–3.4 and $K_{IR}3.1$–3.2 channels in the presence of 90 mM K^+ were also not significantly different (*P* > 0.05; one way ANOVA, followed by Tukey's multiple comparison test; Table 1). This indicates that the activity of naringin at $K_{IR}3.1$–3.4 and $K_{IR}3.1$–3.2 channels is independent of the extracellular K^+ concentration. In all cases, the Hill coefficients (n_H) did not significantly vary between $K_{IR}3.1$–3.4 and $K_{IR}3.1$–3.2 (*P* > 0.05; Table 1).

The EC_{50} and n_H values for naringin on $K_{IR}3.1$–3.4 in the presence and absence of $GABA_{B(1b,2)}$ receptors were not significantly different (*P* > 0.05; one way ANOVA, followed by Tukey's multiple comparison test; Table 1) further indicating that the activation by naringin is not via the $GABA_B$ receptor. Thus, naringin activates $K_{IR}3$ channels independently of the extracellular K^+ concentration and with similar potency at $K_{IR}3.1$–3.4 and $K_{IR}3.1$–3.2 channels.

Naringin activates $K_{IR}3$ channels at an extracellular site

In order to determine whether naringin activated $K_{IR}3$ channels by an extracellular or intracellular site, oocytes
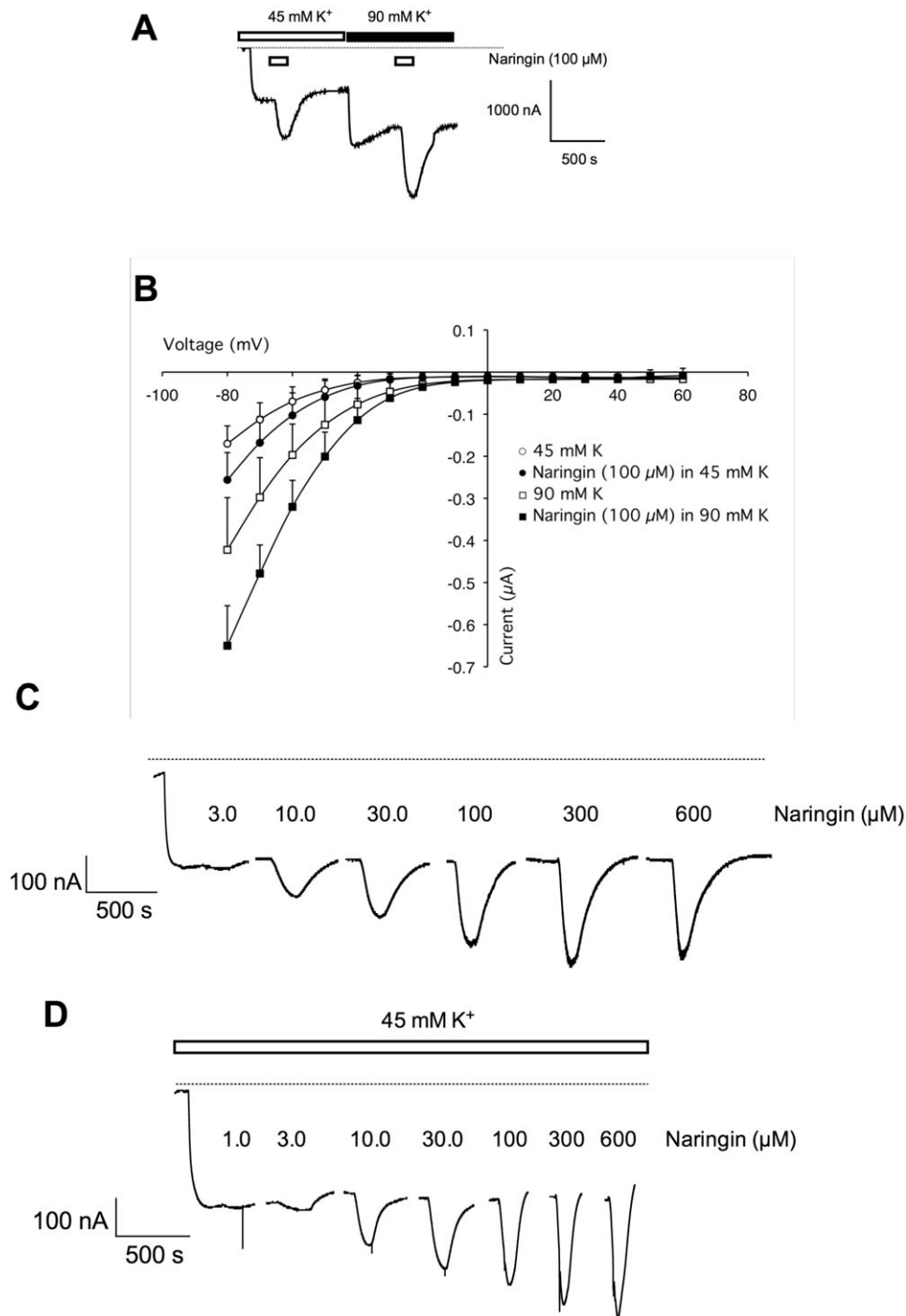
Figure 2

(A) Effect of naringin (100 μM; duration indicated by open bar) on $K_{IR}3.1$–3.4 channels expressed in *Xenopus* oocytes in the presence of 45 mM K⁺ buffer (duration indicated by hatched bar) and 90 mM K⁺ buffer (duration indicated by filled bar), measured at −60 mV. (B) Current–voltage relationship for naringin-sensitive currents generated from wild-type $K_{IR}3.1$–3.4 expressed in *Xenopus* oocytes and measured at 45 and 90 mM K⁺ buffers. Current responses were measured at a holding potential of −30 mV. Currents were measured in a 10 mV increment from −80 to 60 mV in response to 100 ms voltage steps in presence of ND96 buffer, 45 mM K⁺ buffer, naringin (100 μM) in the presence of 45 mM K⁺ buffer, 90 mM K⁺ buffer and naringin (100 μM) in the presence of 90 mM K⁺ buffer. Current–voltage relationships in ND96 buffer were subtracted offline from traces recorded in 45 mM K⁺ buffer, naringin (100 μM) in the presence of 45 mM K⁺ buffer, 90 mM K⁺ buffer and naringin (100 μM) in the presence of 90 mM K⁺ buffer to correct for leak and endogenous oocyte currents. Each voltage point is shown as mean ± SEM of current (μA) from three to six oocytes. (C) Example of an oocyte expressing $K_{IR}3.1$–3.4. In the presence of 45 mM K⁺ naringin generated an outward current when clamped at −60 mV in a concentration-dependent manner. (D) Example of an oocyte expressing $K_{IR}3.1$–3.4. In the presence of 45 mM K⁺ naringin generated outward currents in a concentration-dependent manner when clamped at −60 mV.

Table 1

Effect of naringin on wild-type $K_{IR}3$ channels expressed in *Xenopus* oocytes using two-electrode voltage clamp methods

Channel	$I_{-60 \text{ mV, 45 K}}$ (nA) (n)	Naringin EC$_{50}$ [95% CI] (μM) (logEC$_{50}$ $\pm$ SEM)	$n_H \pm$ SEM	n
$K_{IR}3.1–3.4$	313 $\pm$ 37 (71)	120.9 [69.7–209.8] (2.08 $\pm$ 0.01)	0.93 $\pm$ 0.03	6
	1406 $\pm$ 340 (17)[a]	71.0[a] [55.4–91.0] (1.85 $\pm$ 0.08)	0.84 $\pm$ 0.08	5
	–	91.8[b] [40.2–209.5] (1.96 $\pm$ 0.09)	0.86 $\pm$ 0.18	4
$K_{IR}3.1^{F137S}$	551 $\pm$ 104 (7)	214.7 [81.5–565.7] (2.33 $\pm$ 0.01)	0.86 $\pm$ 0.01	6
$K_{IR}3.4^{S143T}$	350 $\pm$ 124 (11)	104 [71–152] (2.02 $\pm$ 0.08)	1.0 $\pm$ 0.2	6
$K_{IR}3.1–3.2$	583 $\pm$ 71 (50)	111.0 [50.8–242.3] (2.05 $\pm$ 0.08)	0.93 $\pm$ 0.11	4
	823 $\pm$ 127 (23)[a]	58.6[a] [33.0–105.2] (1.77 $\pm$ 0.04)	1.03 $\pm$ 0.07	5

[a]Activity determined using 90 mM K$^+$ buffer.
[b]Coinjected with mRNA of GABA$_{B(1b)}$, GABA$_{B2}$ subunits.
Unless otherwise stated, 45 mM K$^+$ was used for recording.

expressing $K_{IR}3.1–3.4$ channels were first activated by extracellular application of naringin (100 μM). Then naringin (50.6 nL of a 2 mM stock) or water (50.6 nL) was injected into the oocyte. Neither water nor naringin generated a current under these conditions even after a 40 min recording period (Figure 3A and C). In contrast, oocytes expressing $K_{IR}3.1–3.4$ were activated by extracellular and intracellular application of ethanol (100 mM; Figure 3B). Figure 3B shows a sustained activation by ethanol. Taken together the data indicate that naringin activates $K_{IR}3.1–3.4$ channels only at an extracellular site.

The effect of naringin is inhibited by barium

Ba^{2+}, a non-specific K_{IR} channel blocker, significantly inhibited the effect of naringin (100 μM) on $K_{IR}3.1–3.4$ channels in a concentration-dependent manner (Figure 4). Figure 4A shows an example of a trace where Ba^{2+} (100 μM and 3 mM) blocked 80% and 100% the effect of naringin respectively ($P = 0.0001$; Student's t-test; Figure 4B).

The activation of $K_{IR}3$ channels by naringin is not via an endogenous GPCR

To determine whether naringin stimulated an endogenous receptor, we evaluated the binding of naringin to a range of known GPCR/ion channels. Naringin did not bind to any GPCR/ion channel tested to date (Table S2).

In addition to the binding studies, naringin was evaluated on endogenous adenosine receptors known to express in the *Xenopus* oocyte (Kobayashi *et al.*, 2002). In oocytes expressing $K_{IR}3.1–3.4$ channels, adenosine produced a concentration-dependent response by activating $K_{IR}3.1–3.4$ channels via the endogenous receptor. The EC$_{50}$ value obtained for adenosine was 2.7 μM (95% CI = 2.36–3.0) and the n_H was 1.57 $\pm$ 0.07 ($n = 3$; Table 4). In order to determine whether naringin activated this receptor, theophylline (100 μM), a non-selective adenosine receptor antagonist was used. Theophylline (100 μM) blocked the effect of adenosine (1 μM) but did not block the effect of a low concentration of naringin

(10 μM; $n = 3$; Figure S3), indicating that the effects of naringin on recombinant $K_{IR}3.1–3.4$ channels are not via the endogenous adenosine receptor.

Tertiapin-Q competitively inhibited naringin indicating an overlapping binding site

Tertiapin-Q is a potent $K_{IR}1.1$ and $K_{IR}3$ channel blocker (Jin and Lu, 1998; Kanjhan *et al.*, 2005), which binds to the external vestibule of the K$^+$-conduction pore that is formed by the linker between M1 and M2 segments (Ramu *et al.*, 2004) to inhibit the basal current. To determine whether tertiapin-Q inhibits naringin in a competitive or non-competitive manner, we evaluated the effect of naringin alone and in the presence of three concentrations of tertiapin-Q (0.5 nM, 1 nM and 3 nM). We chose low concentrations of tertiapin-Q because we wanted to have maximal inhibition of naringin-stimulated response and minimal basal inhibition. We also compared the effect of GABA alone and in the presence of the maximum concentration of tertiapin-Q (3 nM). Figure 5A and B shows the concentration–response curves for naringin and GABA respectively. Tertiapin-Q shifted the concentration–response curves for naringin to the right (Figure 5A). In addition the Schild slope did not significantly deviate from 1, indicating that tertiapin-Q competitively blocks naringin at $K_{IR}3.1–3.4$ channels. The K_b (binding constant) for tertiapin-Q was found to be 184 $\pm$ 23 pM, 20- to 25-fold more potent than previously reported (Jin and Lu, 1998; Kanjhan *et al.*, 2005). These data infer that tertiapin-Q and naringin share a common or overlapping binding site.

Tertiapin-Q (3 nM) did not shift the concentration–response curve for GABA (Figure 5B). Instead tertiapin-Q inhibited the maximum response to GABA 100 μM (Figure 5C and D). Figure 5C shows a trace of GABA stimulating recombinant GABA$_{B(1b,2)}$ and $K_{IR}3.1–3.4$ channels. When tertiapin-Q (1 μM) was added, the basal response was dramatically reduced. In the presence of tertiapin-Q (1 μM), GABA (100 μM) exerted only 10% of the original response. Figure 5D shows a concentration-dependent inhibition of the GABA (100 μM) response by tertiapin-Q (0, 3, 10 and
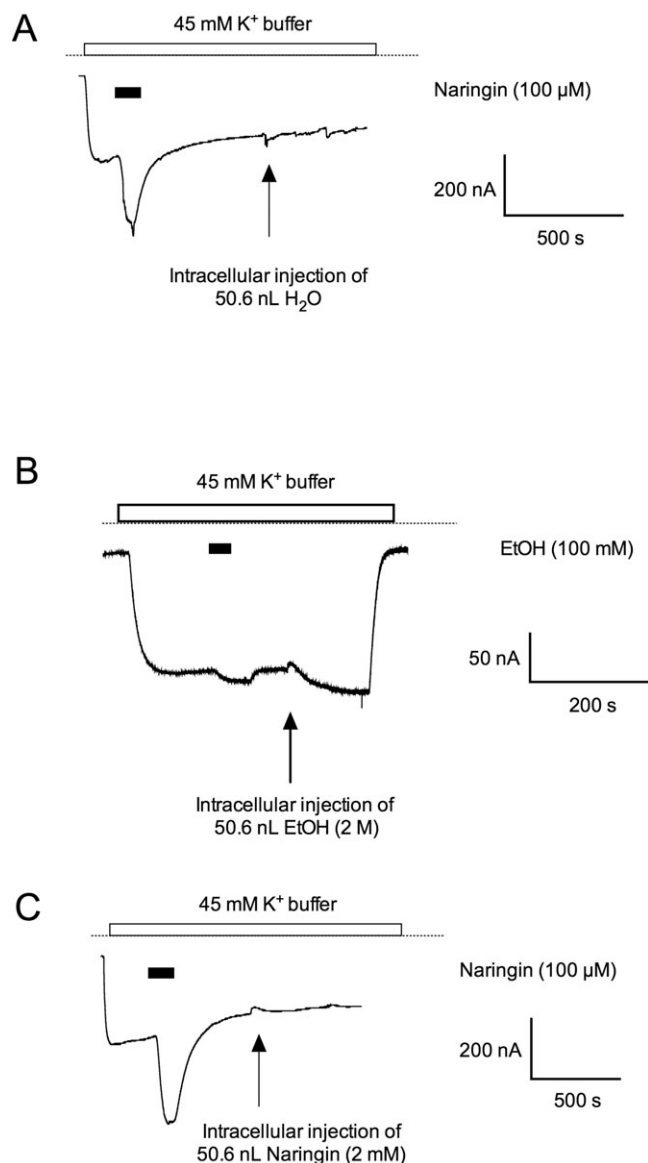
Figure 3

Effects of naringin (100 μM; filled bar) and ethanol (100 mM) when applied extracellularly to *Xenopus* oocytes expressing K$_{IR}$3.1–3.4 channels in the presence of 45 mM K$^+$ buffer (open bar). When either (A) water (50.6 nL; filled bar), (B) ethanol (100 mM–50.6 nL of 2 mM stock solution; filled bar) or (C) naringin (50.6 nL of 2 mM stock solution; filled bar) is injected into the cytoplasm of the oocyte, only ethanol produced a sustained response. No response was observed to water or naringin, indicating that naringin does not act at an intracellular site.

100 nM). The data indicate that tertiapin-Q inhibits GABA in a non-competitive manner.

Effects of naringin and tertiapin-Q on homotetrameric K$_{IR}$3.4^{S143T} and K$_{IR}$3.1^{F137S} mutant channels

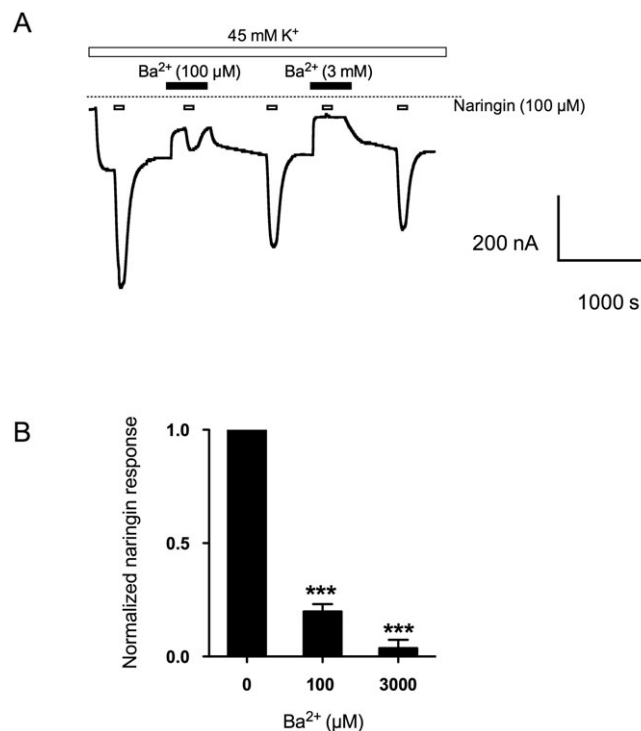If naringin and tertiapin-Q share a common or overlapping binding site, then naringin must bind to one or both K$_{IR}$3

Figure 4

(A) Naringin (100 μM; open bar) activates oocytes expressing K$_{IR}$3.1–3.4 in the presence of 45 mM K$^+$ buffer (open bar). BaCl$_2$ (100 μM and 3 mM; filled bars) inhibited the effect of naringin (100 μM; open bar). (B) Histogram indicating the inhibition by 100 μM and 3 mM BaCl$_2$, respectively, in the presence of naringin (100 μM) alone. Each column represents the mean ($\pm$SEM) of four oocytes from at least two harvests. Statistical significance is as indicated: ***$P < 0.001$.

subunit subtypes that make up the K$_{IR}$3.1–3.4 tetramer. In order to determine which subunit(s) naringin binds to, we evaluated the effects of naringin on the homotetrameric K$_{IR}$3.4^{S143T} and K$_{IR}$3.1^{F137S} mutant channels. Phe137 of K$_{IR}$3.1 is a site for synergy interactions with K$_{IR}$3.2–3.4. Mutating this position to serine, the corresponding amino acid in K$_{IR}$3.4 enables translocation of the protein to the cell surface and facilitates homomeric assembly of the channel (Chan *et al.*, 1996). This feature simplifies the study by allowing us to evaluate the effect of naringin on one subunit without the effect of the other. In contrast, K$_{IR}$3.4 channels can form homotetramers but the currents are much smaller and the mean open time is too fast. Thus by mutating serine 143 to threonine, the resulting mutant channel, K$_{IR}$3.4^{S143T}, produces more robust and sustained currents for the study (Chan *et al.*, 1996).

The basal current of K$_{IR}$3.1^{F137S} in 45 mM K$^+$ was 551 $\pm$ 104 nA ($n = 7$) (Table 1) and naringin further evoked a current of 128 $\pm$ 25 nA ($n = 6$). The EC$_{50}$ and n_H for naringin at K$_{IR}$3.1^{F137S} (Table 1) were not significantly different from wild-type K$_{IR}$3.1–3.4 channels ($P > 0.05$). The basal current of K$_{IR}$3.4^{S143T} in 45 mM K$^+$ was 350 $\pm$ 124 nA ($n = 6$) and naringin further evoked currents of 400 $\pm$ 120 nA ($n = 6$) (Table 1). The EC$_{50}$ and n_H for naringin at K$_{IR}$3.4^{S143T} were not significantly
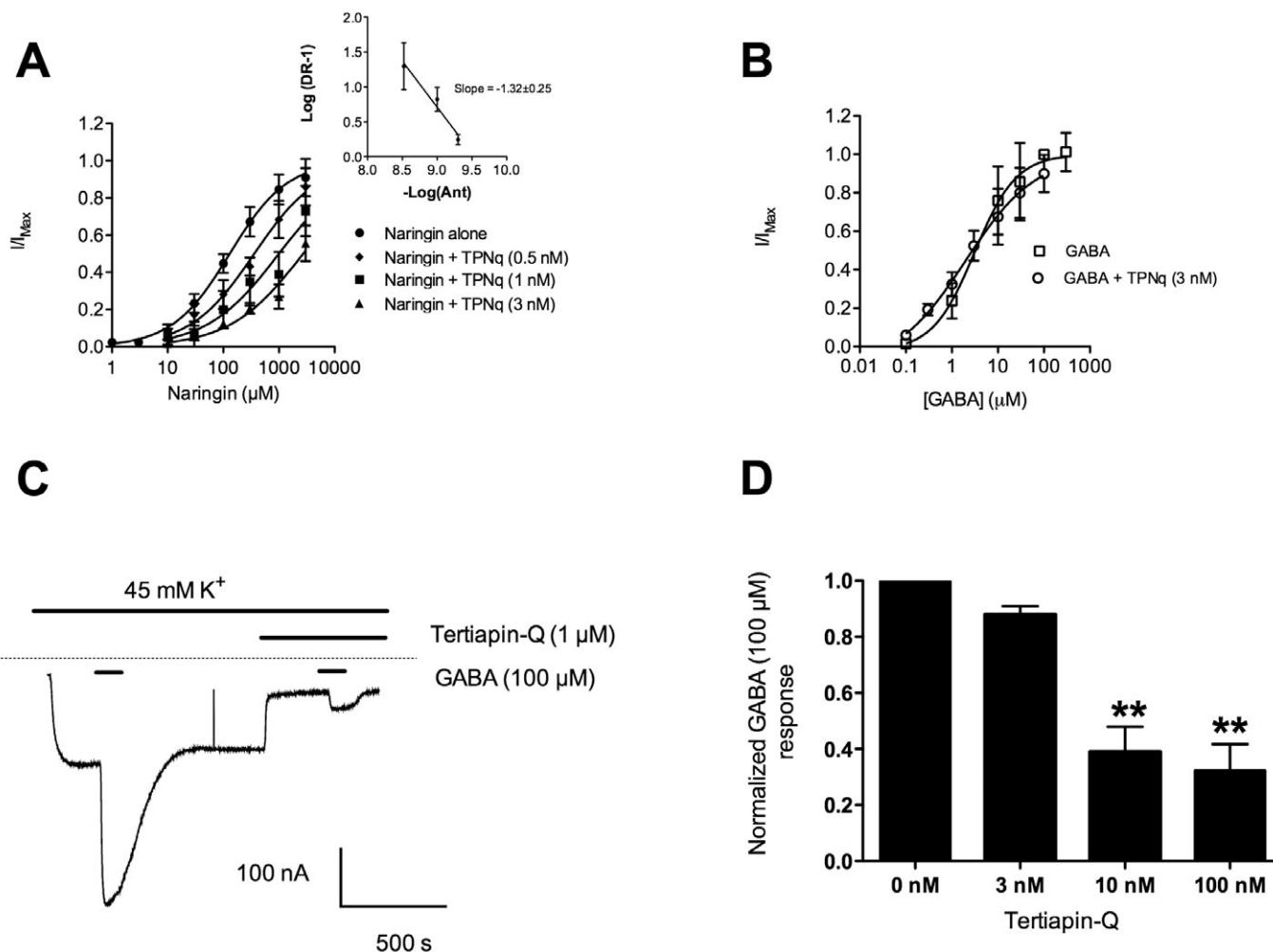
Figure 5

(A) Concentration–response curves for naringin alone, and in the presence of 0.5 nM, 1 nM and 3 nM tertiapin-Q at $K_{IR}3.1$–3.4 channels expressed in oocytes. Tertiapin-Q shifted the EC_{50} of naringin in a parallel manner. The inset shows the curve of log [dose ratio (DR) – 1] versus –log [Ant]. The slope of -1.32 ± 0.25 was not significantly different from 1, indicating competitive antagonism. (B) Concentration–response curve for GABA alone and in the presence of 3 nM tertiapin-Q at $GABA_{B(1b,2)}$ coexpressed with $K_{IR}3.1$–3.4 channels in oocytes. Tertiapin-Q had no effect on the EC_{50} of GABA but started to inhibit the maximal response, indicating non-competitive inhibition. (C) Example trace of an oocyte expressing $GABA_{B(1b,2)}$ and $K_{IR}3.1$–3.4 channels. High K^+ buffer (45 mM K^+) stimulates a basal current, which, in the presence of GABA (100 µM), is further activated. Tertiapin-Q (1 µM) inhibits the basal current by 80%. When tertiapin-Q (1 µM) is applied with GABA (100 µM), the response to GABA is reduced by 90%. Data points are expressed as mean $\pm$ SEM ($n = 4$ oocytes from at least two harvests). (D) Effect of GABA (100 µM) in the presence of various concentrations of tertiapin-Q. Tertiapin-Q reduces the GABA (100 µM) response in a concentration-dependent manner. The concentrations of tertiapin-Q required to inhibit GABA (100 µM) responses were at least 10-fold higher than those inhibiting naringin response. Each column represents the mean ($\pm$SEM) of four oocytes from at least two harvests. Statistical significance is as indicated: ** $P < 0.001$.

different from wild-type $K_{IR}3.1$–3.4 channels ($P > 0.05$; Table 1). Collectively, the data indicate that naringin activates both $K_{IR}3.1^{F137S}$ and $K_{IR}3.4^{S143T}$ subunits with similar potencies compared with wild-type $K_{IR}3.1$–3.4 channels (Figure 6A; Table 1).

In contrast, the effect of tertiapin-Q on $K_{IR}3.1^{F137S}$ was dramatically reduced compared with wild-type $K_{IR}3.1$–3.4 channels. The concentration of tertiapin-Q required to significantly inhibit basal currents generated by the $K_{IR}3.1^{F137S}$ mutant channel was ≥ 3 µM. Figure 6B is an example of a trace where 45 mM K^+ buffer generated a basal response. Ba^{2+}

(1 mM) completely inhibited the basal response but tertiapin-Q (3 nM–3 µM) had little effect. Furthermore, tertiapin-Q (0.5 nM and 3 nM) did not shift the concentration–response curve for naringin on the $K_{IR}3.1^{F137S}$ mutant (Figure 6C). These data indicate that tertiapin-Q does not potently bind to $K_{IR}3.1^{F137S}$ channels and most likely binds with high potency to the $K_{IR}3.4$ subunit. Although it is possible that the F137S mutation alters the binding site of tertiapin-Q but Ramu and colleagues (Ramu *et al.*, 2004) showed that the whole P-loop of $K_{IR}3.1$ is insensitive to tertiapin-Q.
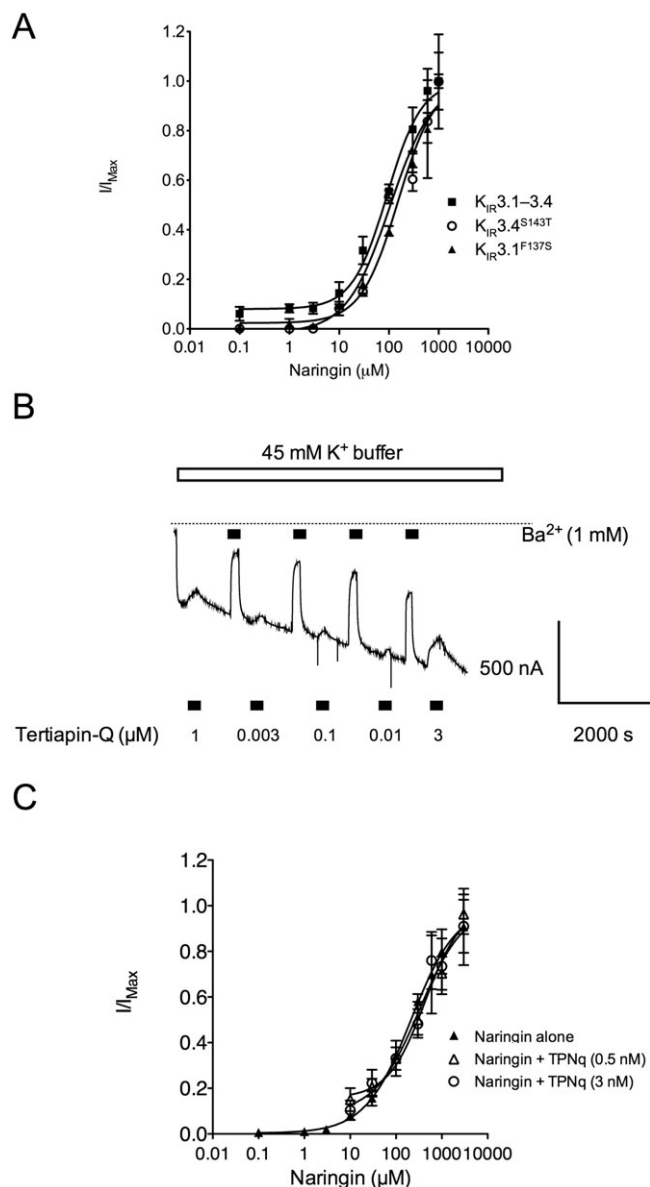
Figure 6

(A) Concentration–response curves for naringin on $K_{IR}3.1$–3.4, $K_{IR}3.4^{S143T}$ and $K_{IR}3.1^{F137S}$ channels expressed in oocytes. No statistical differences were detected in the EC_{50} or n_H for naringin in these channels. (B) A representative trace showing the basal current generated by 45 mM K+ buffer on oocytes expressing $K_{IR}3.1^{F137S}$. Ba^{2+} (1 mM) blocked 90% of the basal current while tertiapin-Q could not block the currents unless the concentration was >1 μM. (C) Concentration–response curves for naringin alone and in the presence of 0.5 nM and 3 nM tertiapin-Q on oocytes expressing $K_{IR}3.1^{F137S}$ channels. Tertiapin-Q could not shift the concentration–response curves of naringin to the right nor could it inhibit the maximal currents indicating naringin is not blocked by tertiapin-Q at $K_{IR}3.1^{F137S}$ channels.

Effects of naringin, GABA, adenosine and LPA on functional $K_{IR}3.1^{F137S}$ double mutants

Nine additional mutations were generated from the $K_{IR}3.1^{F137S}$ mutation: $K_{IR}3.1^{F137SF107A}$, $K_{IR}3.1^{F137SY120A}$, $K_{IR}3.1^{F137SY128A}$,

$K_{IR}3.1^{F137SY130A}$, $K_{IR}3.1^{F137SF134A}$, $K_{IR}3.1^{F137SF136A}$, $K_{IR}3.1^{F137SY146A}$, $K_{IR}3.1^{F137SY148A}$ and $K_{IR}3.1^{F137SY150A}$. These were evaluated in order to identify amino acids important for naringin activity but not GABA activity. By identifying amino acids important for naringin activity on the $K_{IR}3$ channel will further support our hypothesis that naringin directly activates $K_{IR}3$ channels. Tables 2 and 3 summarize the data.

The basal currents observed for the double mutants $K_{IR}3.1^{F137SF130A}$, $K_{IR}3.1^{F137SF134A}$, $K_{IR}3.1^{F137SF136A}$ and $K_{IR}3.1^{F137SY146A}$ did not significantly differ from the basal currents produced by uninjected oocytes in the presence of 45 mM K+, and ranged from 25 to 56 nA (Table 2). Naringin (100 μM) did not further activate oocytes expressing these mutants. In addition Ba^{2+} (3 mM) had no effect at these mutants (data not shown).

The activity of GABA on $GABA_{B(1b,2)}$ and $K_{IR}3.1^{F137S}$ channel expressed in oocytes was not significantly different from wild-type $K_{IR}3.1$–3.4 channels ($P > 0.05$; Table 3). When GABA (100 μM) was tested against the double mutants $K_{IR}3.1^{F137SF130A}$, $K_{IR}3.1^{F137SF134A}$, $K_{IR}3.1^{F137SF136A}$ and $K_{IR}3.1^{F137SY146A}$, it did not further activate oocytes expressing these mutants. The absence of ionic currents regardless of using either GABA or naringin indicates that these amino acids are important for cell surface expression and or channel gating.

Detectable currents in the presence of naringin and GABA were obtained from the double mutants $K_{IR}3.1^{F137SY107A}$, $K_{IR}3.1^{F137SY120A}$, $K_{IR}3.1^{F137SY128A}$, $K_{IR}3.1^{F137SY148A}$ and $K_{IR}3.1^{F137SY150A}$. The basal currents evoked by the double mutants in the presence of 45 mM K+ are summarized in Table 2 and ranged from 62 to 263 nA. In general, these mutants had lower basal currents compared with wild-type $K_{IR}3.1$–3.4 channels. Naringin (100 μM) further evoked currents ranging from 27 to 155 nA (Table 2).

Figure 7 shows the current–voltage (I–V) relationship for naringin from –80 to +80 mV using 45 mM K+ in the absence and presence of naringin (100 μM) mutant GIRK1 channels. The curves indicate all mutant channels are strongly rectified and the effect of naringin on these channels is independent of the voltage. Example traces for naringin (100 μM)-induced responses at wild-type mutant channels are shown as an inset in Figure 7.

Concentration–response curves for naringin were determined for all functional mutants. There were no significant differences in the EC_{50} or n_H for naringin at the double mutants $K_{IR}3.1^{F137SY107A}$, $K_{IR}3.1^{F137SY120A}$ and $K_{IR}3.1^{F137SY128A}$ ($P > 0.05$; Table 2; Figure 8A) when compared with either $K_{IR}3.1^{F137S}$ or wild-type $K_{IR}3.1$–3.4 channels. In contrast, there were significant differences in the n_H and EC_{50} of naringin at $K_{IR}3.1^{F137SY148A}$ and $K_{IR}3.1^{F137SY150A}$ double mutants (Table 2; Figure 8A and B) compared with GIRK1^{F137S} or wild-type GIRK1/4 channels, indicating that Tyr148 and Tyr150 may play a role in either the binding and/or gating of naringin at these channels. The low n_H for naringin at $K_{IR}3.1^{F137SY148A}$ and $K_{IR}3.1^{F137SY150A}$ may also reflect the incomplete concentration–response curve, as the high EC_{50} values may be distorting these figures. Both the EC_{50} and n_H values for naringin on the double mutants $K_{IR}3.1^{F137SY148A}$ and $K_{IR}3.1^{F137SY150A}$ could not be experimentally determined because of solubility problems encountered by naringin at the high concentrations required to complete the concentration–response curves. Instead, EC_{50} and n_H values were calculated by extrapolating the available data using GraphPad Prism v5.0 software. From the extrapo-

Table 2

Effect of naringin on $K_{IR}3.1^{F137S}$ mutants expressed in *Xenopus* oocytes

Channel	$I_{-60\ mV,\ 45\ K}$ (nA) (n)	Naringin (100 µM) (n)	EC$_{50}$ [95% CI] (µM) (logEC$_{50}$ ± SEM)	n_H ± SEM
$K_{IR}3.1^{F137SY107A}$	263 ± 7 (12)	115.5 ± 18 (12)	148.4 [23.8–924.5] (2.17 ± 0.15)	0.58 ± 0.08
$K_{IR}3.1^{F137SY120A}$	161 ± 17 (19)	155.5 ± 25 (19)	84.8 [53.3–134.9] (1.93 ± 0.008)	0.90 ± 0.01
$K_{IR}3.1^{F137SY128A}$	123 ± 9 (17)	64 ± 8 (17)	107.8 [46.6–249.4] (2.03 ± 0.03)	1.02 ± 0.063
$K_{IR}3.1^{F137SF130A}$	36 ± 4 (4)	n.i. (4)	–	–
$K_{IR}3.1^{F137SF134A}$	39 ± 3 (7)	n.i. (6)	–	–
$K_{IR}3.1^{F137SF136A}$	56 ± 10 (9)	n.i. (9)	–	–
$K_{IR}3.1^{F137SY146A}$	25.0 ± 3.5 (5)	n.i. (4)	–	–
$K_{IR}3.1^{F137SY148A}$	181 ± 30 (19)	66 ± 12 (17)	4665[†] (3.67 ± 0.31)***	0.35 ± 0.03###
	185 ± 16 (15)[a]	142 ± 34 (9)	4280[a†] (3.63 ± 0.56)***	0.37 ± 0.06###
$K_{IR}3.1^{F137SY150A}$	62 ± 5 (16)	27.5 ± 2.6 (16)	2849[†] (3.46 ± 0.21)**	0.46 ± 0.04###
	45 ± 4 (20)[a]	35.6 ± 10.9 (13)	2833[a†] (3.45 ± 0.10)**	0.51 ± 0.02##

[a]Coinjected with GABA$_{B(1b)}$, GABA$_{B2}$ subunits.
[†]Concentration–response curve was determined by extrapolating all the available data using Prism 5.0.
***$P < 0.001$, **$P < 0.01$: comparison with $K_{IR}3.1$–3.4 logEC$_{50}$ value (one way ANOVA followed with Tukey's multiple comparison test).
###$P < 0.001$, ##$P < 0.01$: comparison with $K_{IR}3.1$–3.4 n_H value (one way ANOVA followed with Tukey's multiple comparison test).
n.i., no ionic currents detected by naringin (100 µM).

Table 3

Effect of GABA on GABA$_{B(1b,2)}$ receptors coexpressed with wild-type and mutant $K_{IR}3$ channels in *Xenopus* oocytes

Channel	$I_{-60\ mV,\ 45\ K}$ (nA) (n)	GABA (100 µM) (n)	EC$_{50}$ [95% CI] (µM) (logEC$_{50}$ ± SEM) (n)	n_H ± SEM
$K_{IR}3.1$–3.4	252 ± 38.5 (7)	207 ± 28 (7)	3.1 [1.1–8.8] (0.49 ± 0.22) (3–5)	0.93 ± 0.33
$K_{IR}3.1^{F137S}$	777 ± 160 (8)	349 ± 175 (8)	1.43 [0.44–4.7] (0.16 ± 0.13)	0.57 ± 0.11
$K_{IR}3.1^{F137SY107A}$	262 ± 30 (12)	130 ± 42	1.37 [0.5–3.7] (0.14 ± 0.09)	0.61 ± 0.09
$K_{IR}3.1^{F137SY120A}$	155 ± 18 (13)	133 ± 31 (13)	6.71 [3.4–13.1] (0.83 ± 0.05)	0.67 ± 0.06
$K_{IR}3.1^{F137SY128A}$	129 ± 18 (9)	26 ± 9 (9)	2.76 [1.5–5.0] (0.44 ± 0.05)	0.80 ± 0.08
$K_{IR}3.1^{F137SF130A}$	34.8 ± 4 (5)	n.i. (5)	–	–
$K_{IR}3.1^{F137SF134A}$	66.7 ± 4.4 (3)	n.i. (3)	–	–
$K_{IR}3.1^{F137SF136A}$	28.5 ± 3.7 (11)	n.i. (11)	–	–
$K_{IR}3.1^{F137SY146A}$	53 ± 8 (6)	n.i. (4)	–	–
$K_{IR}3.1^{F137SY148A}$	185 ± 16 (15)	153 ± 20 (13)	2.42 [2.0–2.9] (0.38 ± 0.02)	1.23 ± 0.05
$K_{IR}3.1^{F137SY150A}$	45.2 ± 3.9 (20)	33 ± 4 (19)	1.22 [0.76–2.0] (0.087 ± 0.05)	0.94 ± 0.10

n.i., no ionic current was detected by GABA (100 µM).

lated curves, EC$_{50}$ values of 4665 µM and 2861 µM were obtained for naringin at $K_{IR}3.1^{F137SY148A}$ and $K_{IR}3.1^{F137SY150A}$ respectively. Thus the effect of naringin was substantially reduced by approximately 40-fold at $K_{IR}3.1^{F137SY148A}$ when compared with wild-type $K_{IR}3.1$–3.4 channels ($P < 0.001$) and approximately 20-fold when compared with $K_{IR}3.1^{F137S}$ ($P < 0.01$). Furthermore, naringin's effect on $K_{IR}3.1^{F137SY150A}$ was reduced by 20-fold in comparison with wild-type $K_{IR}3.1$–3.4 channels ($P < 0.01$).

There was no significant difference in the activity of naringin at $K_{IR}3.1^{F137SY148A}$ and $K_{IR}3.1^{F137SY150A}$ in the presence or absence of GABA$_B$ receptors [$P > 0.05$; Student's *t*-test (com-

paring logEC$_{50}$ value for each mutant in the presence or absence of GABA$_B$ receptors); Table 2; Figure 8B].

GABA$_{B(1b,2)}$ receptors were also expressed with the $K_{IR}3.1$ double mutants, $K_{IR}3.1^{F137SY107A}$, $K_{IR}3.1^{F137SY120A}$, $K_{IR}3.1^{F137SY128A}$, $K_{IR}3.1^{F137SY148A}$ and $K_{IR}3.1^{F137SY150A}$. Tables 2 and 3 summarize the basal currents generated in the presence of 45 mM K$^+$ (ranging from 35 to 262 nA) and the additional currents evoked by GABA (100 µM) (ranging from 26 to 153 nA).

GABA concentration–response curves were also determined for all functional mutants (Figure 8C). The EC$_{50}$ values for GABA (Table 3) at these mutants were not significantly different from either the single $K_{IR}3.1^{F137S}$ mutant or wild-type
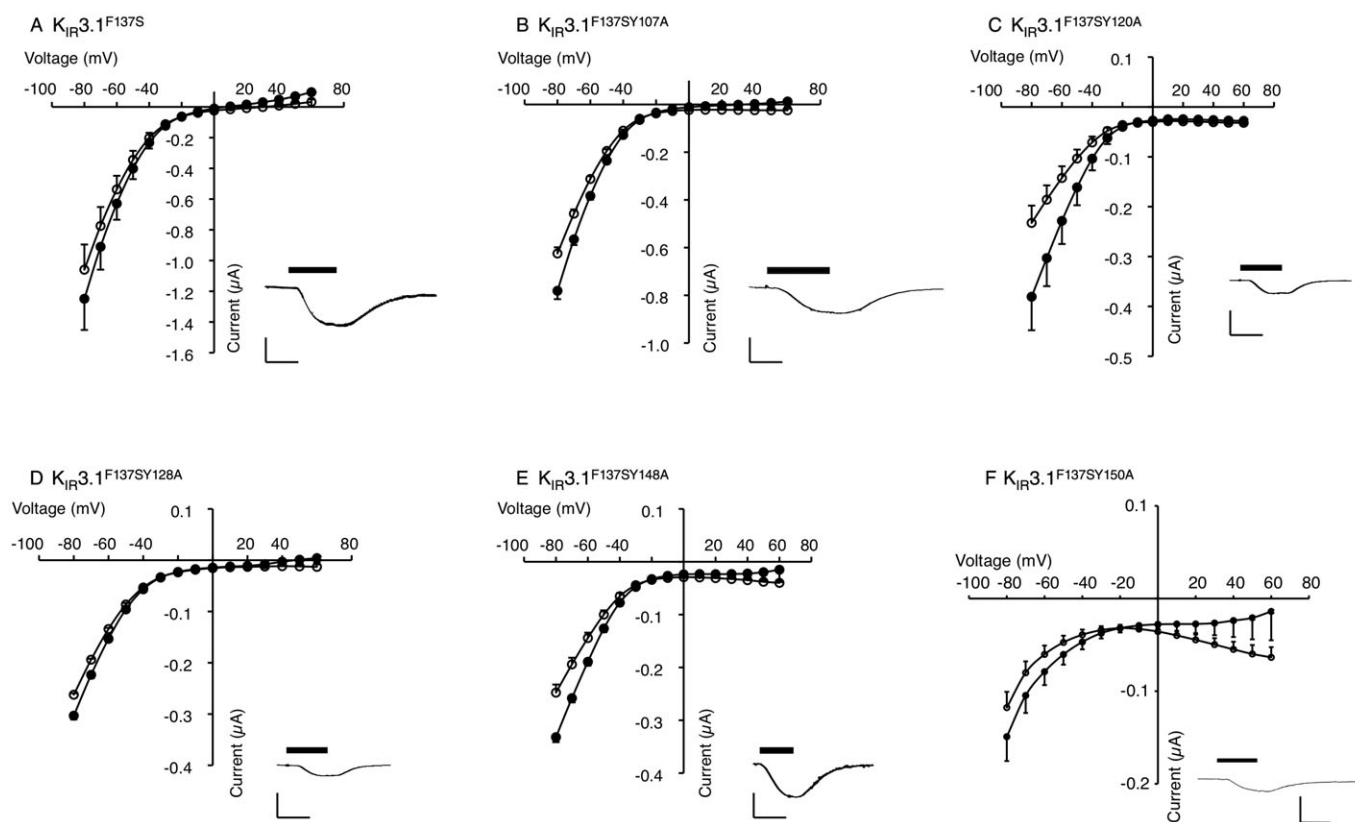
Figure 7

Current–voltage relationship for naringin-sensitive currents. The insets are representative traces of naringin (100 μM)-evoked currents at (A) $K_{IR}3.1^{F137S}$, (B) $K_{IR}3.1^{F137SY107A}$, (C) $K_{IR}3.1^{F137SY120A}$, (D) $K_{IR}3.1^{F137SY128A}$, (E) $K_{IR}3.1^{F137SY148A}$ and (F) $K_{IR}3.1^{F137SY150A}$ mutant channels expressed in *Xenopus* oocytes and measured at 45 mM K^+ buffer. For I–V curves (A) $K_{IR}3.1^{F137S}$, (B) $K_{IR}3.1^{F137SY107A}$, (C) $K_{IR}3.1^{F137SY120A}$, (D) $K_{IR}3.1^{F137SY128A}$, (E) $K_{IR}3.1^{F137SY148A}$ and (F) $K_{IR}3.1^{F137SY150A}$ current responses were measured at a holding potential of −30 mV. Currents were measured in a 10 mV increment from −80 to 60 mV in response to 100 ms voltage steps in the presence of ND96 buffer, 45 mM K^+ buffer (open symbols), and naringin (100 μM) in the presence of 45 mM K^+ buffer (solid symbols). Current–voltage relationships in ND96 buffer were subtracted offline from traces recorded in 45 mM K^+ buffer, and naringin (100 μM) in the presence of 45 mM K^+ buffer to correct for leak and endogenous oocyte currents. Each voltage point is shown as mean ± SEM of current (μA) from three to six oocytes.

Table 4

Effect of stimulating wild-type and mutant $K_{IR}3$ channels expressed in *Xenopus* oocytes by adenosine and LPA through their endogenously expressed receptor

Channel	Adenosine EC$_{50}$ [95% CI] (μM) (logEC$_{50}$ ± SEM)	n_H ± SEM	LPA EC$_{50}$ [95% CI] (nM) (logEC$_{50}$ ± SEM)	n_H ± SEM
$K_{IR}3.1$–3.4	2.66 [2.36–3.0] (0.42 ± 0.01)	1.57 ± 0.01	416 [360–480] (−6.38 ± 0.03)	2.15 ± 0.27
$K_{IR}3.1^{F137SY148A}$	3.60 [2.7–6.3] (0.56 ± 0.02)	1.09 ± 0.05	329 [175–618] (−6.48 ± 0.13)	1.20 ± 0.4
$K_{IR}3.1^{F137SY150A}$	3.10 [1.8–5.4] (0.49 ± 0.06)	1.00 ± 0.12	–	–

$K_{IR}3.1$–3.4 channels ($P > 0.05$) (Figure 8C). Furthermore, the n_H for GABA at $K_{IR}3.1$–3.4 was not statistically different from those obtained from the mutant channels ($P > 0.05$).

To further provide evidence that the $K_{IR}3.1^{F137SY148A}$ and $K_{IR}3.1^{F137SY150A}$ mutants do not affect the affinity of ligands stimulating GPCRs, we evaluated the effects of adenosine and LPA on their prospective receptors expressed endogenously in

oocytes. Adenosine concentration–response curves were constructed for $K_{IR}3.1^{F137SY148A}$ and $K_{IR}3.1^{F137SY150A}$ (Figure 8D) and compared with wild-type $K_{IR}3.1$–3.4. The EC$_{50}$ and n_H values for adenosine at either $K_{IR}3.1^{F137SY148A}$ or $K_{IR}3.1^{F137SY150A}$ were not significantly different from wild-type $K_{IR}3.1$–3.4 ($P > 0.05$; Table 4), indicating that the mutations did not affect adenosine activity.
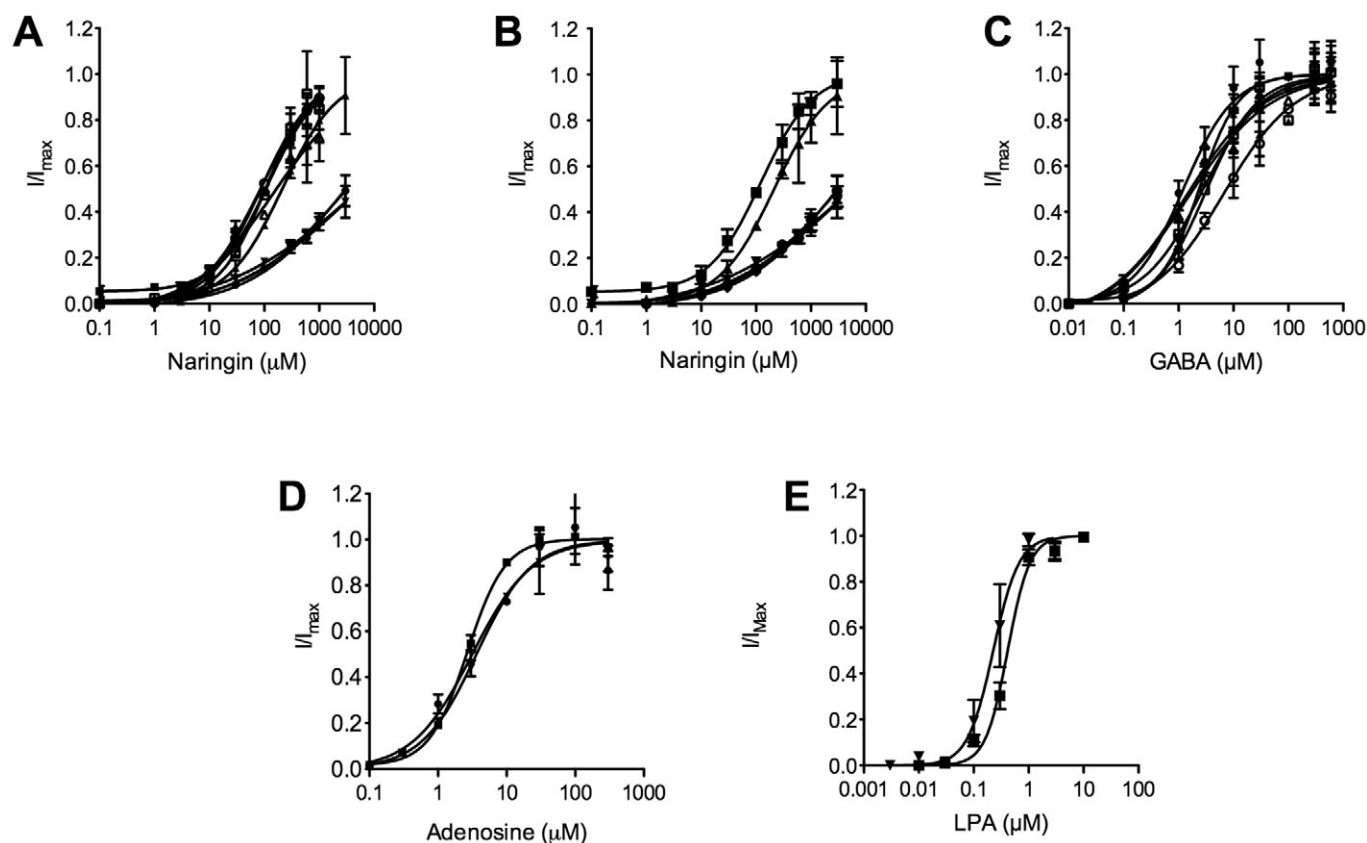
Figure 8

(A) Concentration–response curves for naringin on oocytes expressing $K_{IR}3.1$–3.4 (■), $K_{IR}3.1^{F137S}$ (▲), $K_{IR}3.1^{F137SY107A}$ (△), $K_{IR}3.1^{F137SY120A}$ (○), $K_{IR}3.1^{F137SY128A}$ (□), $K_{IR}3.1^{F137SY148A}$ (▼) and $K_{IR}3.1^{F137SY150A}$ (●). Data points are expressed as mean $\pm$ SEM ($n = 3$–18 oocytes per point from at least two harvests). There is a statistically significant difference in the EC_{50} and Hill coefficient (n_H) values for naringin at $K_{IR}3.1^{F137SY148A}$ and $K_{IR}3.1^{F137SY150A}$ compared with wild-type $K_{IR}3.1$–3.4 and $K_{IR}3.1^{F137S}$ channels (Table 2), indicating that Tyr148 and Tyr150 play a role in the binding and/or gating of naringin at $K_{IR}3$ channels. (B) Concentration–response curves for naringin on oocytes expressing $K_{IR}3.1^{F137S}$, $K_{IR}3.1^{F137SY148A}$, $K_{IR}3.1^{F137SY150A}$ and $GABA_{B(1b,2)}$ with $K_{IR}3.1^{F137SY148A}$ (◆) or $K_{IR}3.1^{F137SY150A}$ (◇). Data points are expressed as mean $\pm$ SEM ($n = 3$–11 oocytes from at least two harvests). There were no significant differences between the EC_{50} or Hill coefficient values for naringin at $K_{IR}3.1^{F137SY148A}$ or $K_{IR}3.1^{F137SY150A}$ in the presence or absence of $GABA_B$ receptors ($P > 0.05$; one-way ANOVA followed by Tukey's *post hoc* test). (C) Concentration–response curves for GABA on oocytes expressing $GABA_{B(1b,2)}$ coupled with either $K_{IR}3.1$–3.4, $K_{IR}3.1^{F137S}$, $K_{IR}3.1^{F137SY107A}$, $K_{IR}3.1^{F137SY120A}$, $K_{IR}3.1^{F137SY128A}$, $K_{IR}3.1^{F137SY148A}$ and $K_{IR}3.1^{F137SY150A}$. Key to symbols used as in (A) and (B). Data points are expressed as mean $\pm$ SEM ($n = 3$–11 oocytes from at least two harvests). There are no significant differences between the EC_{50} or Hill coefficient values for GABA at wild-type $K_{IR}3.1$–3.4 and mutant channels ($P > 0.05$; one-way ANOVA followed by Tukey's *post hoc* test). (D) Concentration–response curves for adenosine on oocytes expressing wild-type $K_{IR}3.1$–3.4, $K_{IR}3.1^{F137SY148A}$ and $K_{IR}3.1^{F137SY150A}$ mutant channels. Data points are expressed as mean $\pm$ SEM ($n = 4$ oocytes per point from at least two harvests). (E) Concentration–response curves for LPA on oocytes expressing wild-type $K_{IR}3.1$–3.4 and $K_{IR}3.1^{F137SY148A}$ mutant channel. Data points are expressed as mean $\pm$ SEM ($n = 3$ oocytes per point from at least two harvests).

The effect of LPA was also evaluated at $K_{IR}3.1^{F137S}$ and $K_{IR}3.1^{F137SY148A}$ channels. We chose to stimulate the LPA receptor because at low LPA concentrations, GIRK channels are activated (Itzhaki Van-Ham *et al.*, 2004) while at high LPA concentrations, Ca^{2+}-activated Cl^- channels are stimulated (Liliom *et al.*, 1996) – reflecting what was observed with naringin in these studies. In oocytes expressing $K_{IR}3.1$–3.4 channels, LPA produced a concentration-dependent response by activating $K_{IR}3.1$–3.4 channels via the endogenous receptor. The EC_{50} and the n_H values for LPA on wild-type $K_{IR}3.1$–3.4 and $K_{IR}3.1^{F137SY148A}$ mutant channels were not significantly different ($P > 0.05$; Figure 8E; Table 4).

Discussion

$K_{IR}3$ channels play an important role in regulating postsynaptic potentials in the central and peripheral nervous systems (Dascal, 1997). Such channels have been implicated in pain perception and in the pathophysiology of several diseases such as epilepsy and ataxia (Luscher and Slesinger, 2010). Agents that can regulate neuronal excitability via $K_{IR}3$ channels through activation, modulation or inhibition have the potential to alleviate pain, reduce increased heart rate associated with arrhythmias and treat epilepsy (Luscher and Slesinger, 2010).

Flavonoids possess many biological actions and exert significant peripheral and central actions such as antihepatotoxic, anti-allergic, anti-inflammatory, anti-osteoporotic, antitumour and neurological activities. Their exact mechanisms of action remain unclear. This study evaluated the effects of the flavonoids, naringin and its aglycosylated analogue (±)-naringenin on recombinant wild-type and mutant $K_{IR}3$ channels expressed in *Xenopus* oocytes. The data presented show that naringin but not (±)-naringenin activates $K_{IR}3$ channels ($K_{IR}3.1$–3.2 and $K_{IR}3.1$–3.4) indicating that the sugar moiety found on the C7 position is important for the activation. Although flavonoids are known to affect many channels including $GABA_A$ receptors (Campbell *et al.*, 2004; Hall *et al.*, 2005; Johnston *et al.*, 2006) and BK_{Ca} channels (Nardi *et al.*, 2003), with few exceptions (Viswanathan *et al.*, 1984; Fernandez *et al.*, 2006; Meotti *et al.*, 2006a,b; 2007; Loscalzo *et al.*, 2008;) most reported studies show that the aglycosylated flavonoids are more effective than their glycosylated counterparts. Of particular significance is the study by Saponara and colleagues who report that (±)-naringenin was more potent than naringin at activating the related BK_{Ca} channels (Saponara *et al.*, 2006).

The activation of $K_{IR}3$ channels generally involves the downstream signalling effectors of *Pertussis* toxin-sensitive GPCRs. Thus, upon GPCR activation by specific neurotransmitters, hormones or peptides, the inactive $G\alpha_{i/o}$-GDP is converted to $G\alpha_{i/o}$-GTP and releases $G\beta\gamma$ subunits from the $G\alpha_{i/o}\beta\gamma$ trimeric complexes. Consequently, the dissociated $G\beta\gamma$ interacts with the GIRK channel C- and N-termini regions leading to channel activation (Dascal, 1997; Yamada *et al.*, 1998; Sadja *et al.*, 2003).

Few substances have been reported to activate $K_{IR}3$ channels via a mechanism that is independent of GPCR stimulation. Only ethanol (Kobayashi *et al.*, 1999) and halothane (Weigl and Schreibmayer, 2001) directly activate $K_{IR}3$ channels. Ethanol activates the channels independently of the $G\alpha_{i/o}$ protein (Kobayashi *et al.*, 1999; Lewohl *et al.*, 1999) and is proposed to act at the C-terminal domain (Lewohl *et al.*, 1999; Hara *et al.*, 2001; Zhou *et al.*, 2001) by either enhancing PIP_2 interactions or by increasing the activity of phosphatidylinositol transfer protein, which could increase the levels of PIP_2 (Zhou *et al.*, 2001). Recently structure-based mutagenesis was used to probe a putative alcohol-binding pocket located in the cytoplasmic domains of $K_{IR}3$ channels (Aryal *et al.*, 2009). The study showed that ethanol could have two binding sites: an activating site and an inhibitory site.

In contrast, halothane is a direct partial inverse agonist on $K_{IR}3$ channels. At low doses (μM range) it inhibits $K_{IR}3$ channels while at high doses (mM range) it activates the channel via allosteric promotion of $G\beta\gamma$ dissociation from the $G\alpha_{i/o}$ protein (Weigl and Schreibmayer, 2001; Milovic *et al.*, 2004). The mechanism by which halothane activates $K_{IR}3$ channels to promote $G\beta\gamma$ dissociation from the $G\alpha_{i/o}$ protein is not known.

In this study, we showed that naringin also activates $K_{IR}3$ channels via a GPCR-independent mechanism and on $K_{IR}3.1$–3.4, the activation was blocked by tertiapin-Q. Tertiapin-Q is a potent blocker of certain K_{IR} including $K_{IR}3.1$–3.2, $K_{IR}3.1$–3.4, the large conductance K^+ channel and G protein-insensitive inwardly rectifying rat $K_{IR}1.1$ channels exhibiting low nanomolar affinity. Mutagenesis studies identified several amino acids important for tertiapin-Q's affinity for $K_{IR}1.1$

activity. These amino acids were located on the external vestibule of the K^+-conduction pore, specifically the M1–M2 linker (Jin *et al.*, 1999). Further evidence to indicate binding of tertiapin-Q occurs at the M1–M2 linker came from studies using the inwardly rectifying $K_{IR}1.1$ channel. $K_{IR}1.1$ is insensitive to tertiapin-Q but when the M1–M2 linker of the $K_{IR}3.4$ but not the $K_{IR}3.1$ subunit was substituted into the $K_{IR}1.1$ subunit, high affinity for the toxin was conferred (Ramu *et al.*, 2004). The affinities reported in these studies for tertiapin-Q at $K_{IR}3$, $K_{IR}1.1_{GIRK4}$ chimeras and $K_{IR}1.1$ channels were determined electrophysiologically measuring channel function. Thus the amount of basal block at any given concentration is assumed to relate to its affinity.

From our studies, we observed that the activation of wild-type $K_{IR}3$ channels by naringin was inhibited by tertiapin-Q in a competitive manner indicating that naringin and tertiapin-Q share a common or overlapping binding site. When measured in this manner, the affinity of tertiapin-Q was found to be 20-fold more potent than previously reported. Thus tertiapin-Q can bind to $K_{IR}3$ channels with high affinity and not affect the basal current, but as the concentration increases the probability of the closed channel state also increases.

Interestingly tertiapin-Q was over 1000-fold weaker at $K_{IR}3.1^{F137S}$ mutant receptors compared with wild-type $K_{IR}3.1$–3.4 receptors, supporting the work by Ramu *et al.* (2004). However as there is no commercially available radioligand, the study by Ramu and colleagues could not differentiate between a gating or binding mechanism. In our studies we evaluated the effect of naringin in the presence and absence of tertiapin-Q on the $K_{IR}3.1^{F137S}$ mutant and found that tertiapin-Q could not inhibit the effect of naringin despite a significant effect on wild-type receptors by the same tertiapin-Q concentration. This indicates that naringin and tertiapin-Q do not share a common binding site on the $K_{IR}3.1$ subunit. Instead, we hypothesize that naringin and tertiapin-Q share an overlapping binding site on the $K_{IR}3.4$ subunit, as naringin does not differentiate between the $K_{IR}3.1$ and $K_{IR}3.4$ subunits, activating both $K_{IR}3.1$ and $K_{IR}3.4$ homomeric channels ($K_{IR}3.1^{F137S}$ and $K_{IR}3.4^{S143T}$) with similar activity.

Important amino acids that confer naringin activity were also identified in this study by performing an alanine-scan of all aromatic amino acids within the M1–M2 linker of the $K_{IR}3.1$ subunit. We chose to mutate aromatic amino acids because the core structure of naringin has two aromatic ring systems, which are likely to interact with aromatic amino acids within the M1–M2 linker region either via π–π and/or hydrophobic interactions. Of the 10 mutations studied, four mutations were not functional: $K_{IR}3.1^{F137SF130A}$, $K_{IR}3.1^{F137SF134A}$, $K_{IR}31^{F137SF136A}$ and $K_{IR}3.1^{F137SY146A}$. The lack of functionality was not altogether surprising as Phe130, 134, 136 and Tyr146 are conserved in the $K_{IR}3$ family. Of particular interest was $K_{IR}3.1^{F137SY146A}$. This mutation is located in the K^+ selectivity filter TIG**Y**G/TIG**F**G (Heginbotham and MacKinnon, 1992; Heginbotham *et al.*, 1992; Doyle *et al.*, 1998), which is highly conserved within the K^+ channel family. Mutating this position in the *Shaker* K^+ channel also knocks out agonist-induced ionic currents (Heginbotham *et al.*, 1994). Thus, this particular mutation was expected to be involved in conductance and indeed this mutation lacked any conductance when stimulated by GABA or naringin.

Jin *et al.* (1999) also found a lack of conductance when they mutated Phe at positions 132 and 134 of the related rat $K_{IR}1.1$ channel to Ala. Phe132 and 134 correspond to Tyr134 and 136 of the $K_{IR}3.1$ channel. As GABA and naringin could not stimulate $K_{IR}3.1^{F137SF134A}$ and $K_{IR}3.1^{F137SF136A}$ channels, the Phe134 and 136 are most likely involved in channel conductance as such positions are conserved throughout the channel family.

In contrast, $K_{IR}3.1^{F137SY107A}$, $K_{IR}3.1^{F137SY120A}$, $K_{IR}3.1^{F137SY128A}$, $K_{IR}3.1^{F137SY148A}$ and $K_{IR}3.1^{F137SY150A}$ formed functional channels. These mutations had, in general, reduced currents: a property that could be attributed to (i) the endogenous $G\alpha$ and $G\beta\gamma$ subunit concentrations, which in this study were not controlled; (ii) $K_{IR}3$ mutant expression levels; and/or (iii) reduced conductivity levels indicating possible changes in channel conformations that lead to the reduced conductivity (Colquhoun, 1998). Reduced conductance or expression levels may interfere with the pharmacodynamic properties of a compound leading to shifts in the EC_{50} values for ligands and possibly observing them to be lower than expected. However, this was not the case as all mutants responded similarly to GABA with no significant changes in GABA, adenosine or LPA activity. Thus, GPCR expression levels (Henry *et al.*, 1995) and the various levels of endogenous $G\alpha$ subunits (Shea *et al.*, 2000; Zhang *et al.*, 2002) within oocyte batches did not contribute to GPCR activity when coupled to the $K_{IR}3.1$ mutants and therefore the mutations had no influence on the way GABA, adenosine or LPA activated the channels. These data are consistent with the hypothesis that naringin binds to the M1–M2 linker of the $K_{IR}3$ channel, a site distinct from direct G protein interactions and that Tyr148 and 150 may play a role in either the binding and or gating of naringin at $K_{IR}3$ channels.

Interestingly in the study by Jin and colleagues, a number of amino acids within the M1–M2 linker of $K_{IR}1.1$ that affected the affinity of tertiapin-Q were identified (Jin *et al.*, 1999), including Phe146 and 148. Phe146 and 148 of rat $K_{IR}1.1$ form part of the external vestibule of the ion conduction pore and when the rat $K_{IR}1.1$ sequence is aligned against the $K_{IR}3.1$ subunit, the phenylalanines correspond to Tyr148 and 150 of the $K_{IR}3.1$ channel. The fact that both Phe146 and 148 of rat $K_{IR}1.1$ and Tyr148 and 150 of $K_{IR}3.1$ subunits affect the affinities of tertiapin-Q and naringin, respectively, indicates the importance of these positions for possible ligand–channel interactions.

Despite the vast knowledge on the structure of the $K_{IR}3$ channel, the pharmacology of this channel family remains largely undeveloped. This study highlights naringin as a lead molecule to further develop into direct activators of the channel. However, naringin cannot act as a drug *per se*: flavonoid glycosides such as naringin are readily metabolized to the aglycone by microflora in the intestine (Manach *et al.*, 2004). Furthermore, naringin exhibits low uptake by intestinal Caco-2 cells (Tourniaire *et al.*, 2005). This indicates that only trace amounts of naringin (approximately 0.5% of ingested naringin) are available in plasma when taken orally (Ishii *et al.*, 2000) and may not be able to reach target sites such as the heart and brain where $K_{IR}3$ channels are expressed. However, when given i.p., naringin exerts sedative (Fernandez *et al.*, 2006) and anxiolytic (Fernandez *et al.*, 2009) effects in mice. This does not accord with the results

from microdialysis studies that show no detectable levels of naringin in rat brain after administration of 30 mg·kg^{-1}, i.p. (Tsai, 2002). However, in the same study it was shown that in the presence of a P-glycoprotein blocker (Tsai, 2002) naringin concentrations are increased in the brain. However, naringin is an example of a generic activator of $K_{IR}3$ channels being equipotent on $K_{IR}3.1$–3.2 and $K_{IR}3.1$–3.4. Only compounds acting on specific $K_{IR}3$ isoforms may be of therapeutic value. The full elucidation of the naringin binding site will aid in the development of such agents.

In conclusion, our study shows that naringin activates $K_{IR}3$ channels by binding to the M1–M2 linker of the $K_{IR}3.1$ and $K_{IR}3.4$ subunits. Mutagenesis studies on the $K_{IR}3.1^{F137S}$ showed that Tyr148 and Tyr150 may be involved in naringin's effects suggesting that channel–ligand interactions may occur via π–π interactions. As tertiapin-Q can completely inhibit naringin at $K_{IR}3.1$–3.4 channels in a competitive manner, they must share a common or overlapping binding site, hypothesized to be at a site on the $K_{IR}3.4$ subunit.

Acknowledgements

Conflict of interest

The authors have no conflict of interest.

References

Alexander SPH, Mathie A, Peters JA (2009). Guide to Receptors and Channels (GRAC), 4th edn. Br J Pharmacol 158: S1–S239.

Aryal P, Dvir H, Choe S, Slesinger PA (2009). A discrete alcohol pocket involved in GIRK channel activation. Nat Neurosci 12: 988–995.

Benians A, Nobles M, Hosny S, Tinker A (2005). Regulators of G-protein signaling form a quaternary complex with the agonist, receptor, and G-protein – a novel explanation for the acceleration of signaling activation kinetics. J Biol Chem 280: 13383–13394.

Birt DF, Hendrich S, Wang W (2001). Dietary agents in cancer prevention: flavonoids and isoflavonoids. Pharmacol Ther 90: 157–177.

Campbell EL, Chebib M, Johnston GA (2004). The dietary flavonoids apigenin and (-)-epigallocatechin gallate enhance the positive modulation by diazepam of the activation by GABA of recombinant GABA$_A$ receptors. Biochem Pharmacol 68: 1631–1638.

Chan KW, Sui JL, Vivaudou M, Logothetis DE (1996). Control of channel activity through a unique amino acid residue of a G protein-gated inwardly rectifying K$^+$ channel subunit. Proc Natl Acad Sci USA 93: 14193–14198.

Colquhoun D (1998). Binding, gating, affinity and efficacy: the interpretation of structure-activity relationships for agonists and of the effects of mutating receptors. Br J Pharmacol 125: 924–947.

Corey S, Clapham DE (1998). Identification of native atrial G-protein-regulated inwardly rectifying K^+ (GIRK4) channel homomultimers. J Biol Chem 273: 27499–27504.

Dascal N (1997). Signalling via the G protein-activated K^+ channels. Cell Signal 9: 551–573.

Doyle DA, Morais Cabral J, Pfuetzner RA, Kuo A, Gulbis JM, Cohen SL et al. (1998). The structure of the potassium channel: molecular basis of K^+ conduction and selectivity. Science 280: 69–77.

Fernandez SP, Wasowski C, Loscalzo LM, Granger RE, Johnston GA, Paladini AC et al. (2006). Central nervous system depressant action of flavonoid glycosides. Eur J Pharmacol 539: 168–176.

Fernandez SP, Nguyen M, Yow TT, Chu C, Johnston GA, Hanrahan JR et al. (2009). The flavonoid glycosides, myricitrin, gossypin and naringin exert anxiolytic action in mice. Neurochem Res 34: 1867–1875.

Gregerson KA, Flagg TP, O'Neill TJ, Anderson M, Lauring O, Horel JS et al. (2001). Identification of G protein-coupled, inward rectifier potassium channel gene products from the rat anterior pituitary gland. Endocrinology 142: 2820–2832.

Hall BJ, Chebib M, Hanrahan JR, Johnston GA (2005). 6-Methylflavanone, a more efficacious positive allosteric modulator of γ-aminobutyric acid (GABA) action at human recombinant $\alpha_2\beta_2\gamma_{2L}$ than at $\alpha_1\beta_2\gamma_{2L}$ and $\alpha_1\beta_2$ GABA$_A$ receptors expressed in Xenopus oocytes. Eur J Pharmacol 512: 97–104.

Hara K, Lewohl JM, Yamakura T, Harris RA (2001). Mutational analysis of ethanol interactions with G-protein-coupled inwardly rectifying potassium channels. Alcohol 24: 5–8.

Heginbotham L, MacKinnon R (1992). The aromatic binding site for tetraethylammonium ion on potassium channels. Neuron 8: 483–491.

Heginbotham L, Abramson T, MacKinnon R (1992). A functional connection between the pores of distantly related ion channels as revealed by mutant K^+ channels. Science 258: 1152–1155.

Heginbotham L, Lu Z, Abramson T, MacKinnon R (1994). Mutations in the K^+ channel signature sequence. Biophys J 66: 1061–1067.

Henry DJ, Grandy DK, Lester HA, Davidson N, Chavkin C (1995). κ-opioid receptors couple to inwardly rectifying potassium channels when coexpressed by Xenopus oocytes. Mol Pharmacol 47: 551–557.

Hertog MG, Kromhout D, Aravanis C, Blackburn H, Buzina R, Fidanza F et al. (1995). Flavonoid intake and long-term risk of coronary heart disease and cancer in the seven countries study. Arch Intern Med 155: 381–386.

Ikeda K, Kobayashi T, Ichikawa T, Usui H, Kumanishi T (1995). Functional couplings of the δ- and the κ-opioid receptors with the G-protein-activated K^+ channel. Biochem Biophys Res Commun 208: 302–308.

Ikeda K, Kobayashi T, Ichikawa T, Usui H, Abe S, Kumanishi T (1996). Comparison of the three mouse G-protein-activated K^+ (GIRK) channels and functional couplings of the opioid receptors with the GIRK1 channel. Ann NY Acad Sci 801: 95–109.

Ikeda K, Kobayashi K, Kobayashi T, Ichikawa T, Kumanishi T, Kishida H et al. (1997). Functional coupling of the nociceptin/orphanin FQ receptor with the G-protein-activated K^+ (GIRK) channel. Brain Res Mol Brain Res 45: 117–126.

Ishii K, Furuta T, Kasuya Y (2000). Mass spectrometric identification and high-performance liquid chromatographic determination of a flavonoid glycoside naringin in human urine. J Agric Food Chem 48: 56–59.

Itzhaki Van-Ham I, Peleg S, Dascal N, Shapira H, Oron Y (2004). G protein-activated K+ channels: a reporter for rapid activation of G proteins by lysophosphatidic acid in Xenopus oocytes. FEBS Lett 564: 157–160.

Jin W, Lu Z (1998). A novel high-affinity inhibitor for inward-rectifier K^+ channels. Biochemistry 37: 13291–13299.

Jin W, Klem AM, Lewis JH, Lu Z (1999). Mechanisms of inward-rectifier K^+ channel inhibition by tertiapin-Q. Biochemistry 38: 14294–14301.

Johnston GA, Hanrahan JR, Chebib M, Duke RK, Mewett KN (2006). Modulation of ionotropic GABA receptors by natural products of plant origin. Adv Pharmacol 54: 285–316.

Kandaswami C, Perkins E, Soloniuk DS, Drzewiecki G, Middleton E Jr (1991). Antiproliferative effects of citrus flavonoids on a human squamous cell carcinoma in vitro. Cancer Lett 56: 147–152.

Kanjhan R, Coulson EJ, Adams DJ, Bellingham MC (2005). Tertiapin-Q blocks recombinant and native large conductance K^+ channels in a use-dependent manner. J Pharmacol Exp Ther 314: 1353–1361.

Kobayashi T, Ikeda K, Ichikawa T, Abe S, Togashi S, Kumanishi T (1995). Molecular cloning of a mouse G-protein-activated K^+ channel (mGIRK1) and distinct distributions of three GIRK (GIRK1, 2 and 3) mRNAs in mouse brain. Biochem Biophys Res Commun 208: 1166–1173.

Kobayashi T, Ikeda K, Kojima H, Niki H, Yano R, Yoshioka T et al. (1999). Ethanol opens G-protein-activated inwardly rectifying K^+ channels. Nat Neurosci 2: 1091–1097.

Kobayashi T, Ikeda K, Kumanishi T (2000). Inhibition by various antipsychotic drugs of the G-protein-activated inwardly rectifying K^+ (GIRK) channels expressed in Xenopus oocytes. Br J Pharmacol 129: 1716–1722.

Kobayashi T, Ikeda K, Kumanishi T (2002). Functional characterization of an endogenous Xenopus oocyte adenosine receptor. Br J Pharmacol 135: 313–322.

Kobayashi T, Washiyama K, Ikeda K (2003). Inhibition of G protein-activated inwardly rectifying K^+ channels by fluoxetine (Prozac). Br J Pharmacol 138: 1119–1128.

Kobayashi T, Washiyama K, Ikeda K (2004). Modulators of G protein-activated inwardly rectifying K^+ channels: potentially therapeutic agents for addictive drug users. Ann NY Acad Sci 1025: 590–594.

Lesage F, Duprat F, Fink M, Guillemare E, Coppola T, Lazdunski M et al. (1994). Cloning provides evidence for a family of inward rectifier and G-protein coupled K^+ channels in the brain. FEBS Lett 353: 37–42.

Lesage F, Guillemare E, Fink M, Duprat F, Heurteaux C, Fosset M et al. (1995). Molecular properties of neuronal G-protein-activated inwardly rectifying K^+ channels. J Biol Chem 270: 28660–28667.

Lewohl JM, Wilson WR, Mayfield RD, Brozowski SJ, Morrisett RA, Harris RA (1999). G-protein-coupled inwardly rectifying potassium channels are targets of alcohol action. Nat Neurosci 2: 1084–1090.

Liliom K, Murakami-Murofushi K, Kobayashi S, Murofushi H, Tigyi G (1996). Xenopus oocytes express multiple receptors for LPA-like lipid mediators. Am J Physiol 270 (3 Pt 1): C772–C777.

Logothetis DE, Zhang H (1999). Gating of G protein-sensitive inwardly rectifying K+ channels through phosphatidylinositol 4,5-bisphosphate. J Physiol 520 (Pt 3): 630.

Loscalzo LM, Wasowski C, Paladini AC, Marder M (2008). Opioid receptors are involved in the sedative and antinociceptive effects of hesperidin as well as in its potentiation with benzodiazepines. Eur J Pharmacol 580: 306–313.

Luscher C, Slesinger PA (2010). Emerging roles for G protein-gated inwardly rectifying potassium (GIRK) channels in health and disease. Nat Rev Neurosci 11: 301–315.

Luscher C, Jan LY, Stoffel M, Malenka RC, Nicoll RA (1997). G protein-coupled inwardly rectifying K+ channels (GIRKs) mediate postsynaptic but not presynaptic transmitter actions in hippocampal neurons. Neuron 19: 687–695.

Manach C, Scalbert A, Morand C, Remesy C, Jimenez L (2004). Polyphenols: food sources and bioavailability. Am J Clin Nutr 79: 727–747.

Mandel S, Youdim MBH (2004). Catechin polyphenols: neurodegeneration and neuroprotection in neurodegenerative diseases. Free Radic Biol Med 37: 304–317.

Mark MD, Herlitze S (2000). G-protein mediated gating of inward-rectifier K+ channels. Eur J Biochem 267: 5830–5836.

Mattila P, Astola J, Kumpulainen J (2000). Determination of flavonoids in plant material by HPLC with diode-array and electro-array detections. J Agric Food Chem 48: 5834–5841.

Meotti FC, Luiz AP, Pizzolatti MG, Kassuya CA, Calixto JB, Santos AR (2006a). Analysis of the antinociceptive effect of the flavonoid myricitrin: evidence for a role of the L-arginine-nitric oxide and protein kinase C pathways. J Pharmacol Exp Ther 316: 789–796.

Meotti FC, Missau FC, Ferreira J, Pizzolatti MG, Mizuzaki C, Nogueira CW et al. (2006b). Anti-allodynic property of flavonoid myricitrin in models of persistent inflammatory and neuropathic pain in mice. Biochem Pharmacol 72: 1707–1713.

Meotti FC, Fachinetto R, Maffi LC, Missau FC, Pizzolatti MG, Rocha JB et al. (2007). Antinociceptive action of myricitrin: involvement of the K+ and Ca²⁺ channels. Eur J Pharmacol 567: 198–205.

Miller JR (2003). GraphPad Prism Version 4.0 Step by Step Examples. GraphPad Software Inc.: San Diego, CA.

Milovic S, Steinecker-Frohnwieser B, Schreibmayer W, Weigl LG (2004). The sensitivity of G protein-activated K+ channels toward halothane is essentially determined by the C terminus. J Biol Chem 279: 34240–34249.

Nardi A, Calderone V, Chericoni S, Morelli I (2003). Natural modulators of large-conductance calcium-activated potassium channels. Planta Med 69: 885–892.

Nichols CG, Lopatin AN (1997). Inward rectifier potassium channels. Annu Rev Physiol 59: 171–191.

Nishida M, MacKinnon R (2002). Structural basis of inward rectification: cytoplasmic pore of the G protein-gated inward rectifier GIRK1 at 1.8 A resolution. Cell 111: 957–965.

Ramu Y, Klem AM, Lu Z (2004). Short variable sequence acquired in evolution enables selective inhibition of various inward-rectifier K+ channels. Biochemistry 43: 10701–10709.

Renaud S, de Lorgeril M (1992). Wine, alcohol, platelets, and the French paradox for coronary heart disease. Lancet 339: 1523–1526.

Sadja R, Alagem N, Reuveny E (2003). Gating of GIRK channels: details of an intricate, membrane-delimited signaling complex. Neuron 39: 9–12.

Saponara S, Testai L, Iozzi D, Martinotti E, Martelli A, Chericoni S et al. (2006). (+/-)-Naringenin as large conductance Ca²⁺ -activated K⁺(BK_Ca) channel opener in vascular smooth muscle cells. Br J Pharmacol 149: 1013–1021.

Shea LD, Neubig RR, Linderman JJ (2000). Timing is everything the role of kinetics in G protein activation. Life Sci 68: 647–658.

Signorini S, Liao YJ, Duncan SA, Jan LY, Stoffel M (1997). Normal cerebellar development but susceptibility to seizures in mice lacking G protein-coupled, inwardly rectifying K⁺ channel GIRK2. Proc Natl Acad Sci USA 94: 923–927.

Sui JL, Petit-Jacques J, Logothetis DE (1998). Activation of the atrial KACh channel by the betagamma subunits of G proteins or intracellular Na+ ions depends on the presence of phosphatidylinositol phosphates. Proc Natl Acad Sci USA 95: 1307–1312.

Tourniaire F, Hassan M, Andre M, Ghiringhelli O, Alquier C, Amiot MJ (2005). Molecular mechanisms of the naringin low uptake by intestinal Caco-2 cells. Mol Nutr Food Res 49: 957–962.

Tsai TH (2002). Determination of naringin in rat blood, brain, liver, and bile using microdialysis and its interaction with cyclosporin a, a p-glycoprotein modulator. J Agric Food Chem 50: 6669–6674.

Ulens C, Daenens P, Tytgat J (1999). The dual modulation of GIRK1/GIRK2 channels by opioid receptor ligands. Eur J Pharmacol 385: 239–245.

Varecka L, Peterajova E (1990). Activation of red-cell Ca-2+-activated K+-channel by Ca-2+ involves a temperature-dependent step. FEBS Lett 276: 169–171.

Viswanathan S, Sambantham PT, Reddy K, Kameswaran L (1984). Gossypin-induced analgesia in mice. Eur J Pharmacol 98: 289–291.

Weigl LG, Schreibmayer W (2001). G protein-gated inwardly rectifying potassium channels are targets for volatile anesthetics. Mol Pharmacol 60: 282–289.

Wickman K, Nemec J, Gendler SJ, Clapham DE (1998). Abnormal heart rate regulation in GIRK4 knockout mice. Neuron 20: 103–114.

Yamada M, Inanobe A, Kurachi Y (1998). G protein regulation of potassium ion channels. Pharmacol Rev 50: 723–760.

Yamakura T, Lewohl JM, Harris RA (2001). Differential effects of general anesthetics on G protein-coupled inwardly rectifying and other potassium channels. Anesthesiology 95: 144–153.

Zhang Q, Pacheco MA, Doupnik CA (2002). Gating properties of GIRK channels activated by Gα_o and Gα_i-coupled muscarinic m2 receptors in Xenopus oocytes: the role of receptor precoupling in RGS modulation. J Physiol 545: 355–373.

Zhou W, Arrabit C, Choe S, Slesinger PA (2001). Mechanism underlying bupivacaine inhibition of G protein-gated inwardly rectifying K⁺ channels. Proc Natl Acad Sci USA 98: 6482–6487.

Supporting information

Additional Supporting Information may be found in the online version of this article:

Figure S1 Ca²⁺-activated Cl⁻ channel activity elicited by naringin in (A) ND96 and (B) 45 mM K⁺ buffer. The distinctive

sharp inward currents were removed by 11 mM EGTA in the intracellular pipettes. Current responses that contained the distinctive sharp inward current were discarded from further analysis. (C) Current voltage relationship for GIRK 1/4 wild-type channels in the presence of 45 mM K^+ buffer with (○) and without (□) 11 mM EGTA in the pipette solution, and in the presence of 100 μM naringin in 45 mM K^+ buffer with (●) and without (■) 11 mM EGTA in the pipette solution. The residual current at ND96 is subtracted from the measured current, and each cell is then normalised to the current at −100 mV.

Figure S2 (A) Effect of a maximum concentration of GABA (100 μM; filled bar), submaximal concentration of GABA (3 μM; open bar) and naringin (100 μM; backward hatched bar) on $GABA_{B(1b,2)}$ receptors coupled to GIRK1/4 channels expressed in *Xenopus* oocytes in the presence of 45 mM K^+ buffer (open bar). CGP36742 (100 μM; forward hatched bar), a competitive $GABA_B$ receptor antagonist inhibited the response of GABA (3 μM; open bar) but not naringin (100 μM; backward hatched bar). (B) Effect of naringin (100 μM; duration indicated by filled bar) activating the channel whereas (±)-naringenin (100 μM; duration indicated by filled bar) and the sugar moiety, neohesperidose (100 μM; duration indicated by solid bar) had no effect on GIRK1/4 channels expressed in oocytes in the presence of 45 mM K^+ buffer (duration indicated by open bar). (C) Effect of naringin (100 μM; duration indicated by filled bar) activating the channel whereas (±)-naringenin (100 μM; duration indicated by filled bar) and the sugar moiety, neohesperidose (100 μM; duration indicated by filled bar) had no effect on GIRK1/2 channels expressed in oocytes in the presence of 45 mM K^+ buffer (duration indicated by open bar).

Figure S3 An example of a trace showing naringin (100 μM; duration indicated by black bar), naringin (10 μM; duration indicated by white bar) and adenosine (1 μM; duration indicated by white bar) evoked currents. Theophylline (100 μM; duration indicated by black bar) blocks the response by adenosine but not naringin at 10 μM.

Table S1 Sense oligonucleotide primers (from 5′ to 3′)

Table S2 Summary of the binding results for naringin (10 μM)

Please note: Wiley-Blackwell are not responsible for the content or functionality of any supporting materials supplied by the authors. Any queries (other than missing material) should be directed to the corresponding author for the article.